

## Response to Referee Dr. Huisheng Bian

(Note: Reviewer comments are listed in grey, and responses to reviewer comments are in black. Pasted text from the new version of the paper is in italics.)

The authors investigated source attribution to the Pacific Ocean using a global chemical transport model MOZART-4 by tagging BC tracer to 13 source regions around the globe. They further quantified the aging timescales of those tagged BC tracers by constraining simulation with aircraft measurements from five HIPPO missions. This is a scientifically interesting study. Publications of AeroCom and other works have demonstrated that many global models currently overestimate BC in free and upper troposphere. This study points out a direction to solve this common problem in modeling global BC field. The paper is well written. I recommend publishing the paper on ACP after the authors make some minor modifications.

We really appreciate the thoughtful and valuable comments from Dr. Bian. It substantially helps to improve our manuscript by addressing these issues.

General Remarks: The authors summarized BC aging timescales associated to 13 source regions. The conclusion is instructive but may be not robust. The authors showed an improved BC simulation by MOZART-4 at current condition with this varying BC aging timescale. But can these aging timescales still be valuable if BC emission and atmospheric oxidant fields are changed in the future in MOZART-4? Can other models apply these adjusted BC aging timescales with some cautions? It may be more useful that the authors explore the key factors that control BC aging, such as emission types, oxidant fields, etc, and parameterize BC aging timescale based on these key factors.

This is an important remark. We agree with the reviewer that investigating the key factors that control aging processes, and developing aging schemes according to these factors will be more useful for future modeling studies. Following the reviewer's comments, we further analyze the spatiotemporal pattern of the optimized aging timescales and re-evaluate the parameterization of BC aging scheme developed by Liu et al (2011) , in which aging rate  $k_a = \beta \cdot [OH] + \gamma$ , is controlled by OH concentration (molecules  $m^{-3}$ ) and two parameters  $\beta$  and  $\gamma$  . After conducting a number of sensitivity tests based on our optimized aging timescales, we find a larger value of parameters  $\beta$  ( $2.4 \times 10^{-11}$ ) and  $\gamma$  ( $1 \times 10^{-6}$ ) can fit well the HIPPO observations. The description of this scheme is added in Section 3:

*"...In this study, we further improve the parameterization of Liu et al. (2011) by finding best-fit values for constants that best match HIPPO observations with reference to our BC aging timescales. After conducting additional sensitivity simulations, we find that a set of parameters (i.e.,  $\beta=2.4 \times 10^{-11}$ , and  $\gamma=1 \times 10^{-6}$  in Equation (4) in Liu et al. (2011)) when employed in*

MOZART-4 can fit well the HIPPO observations as well as ground observations (see Figure S1 and S2 in supplementary material).”

We also evaluated the model with OH-dependent scheme. Please see Figure S1 and S2 in supplementary material or below:

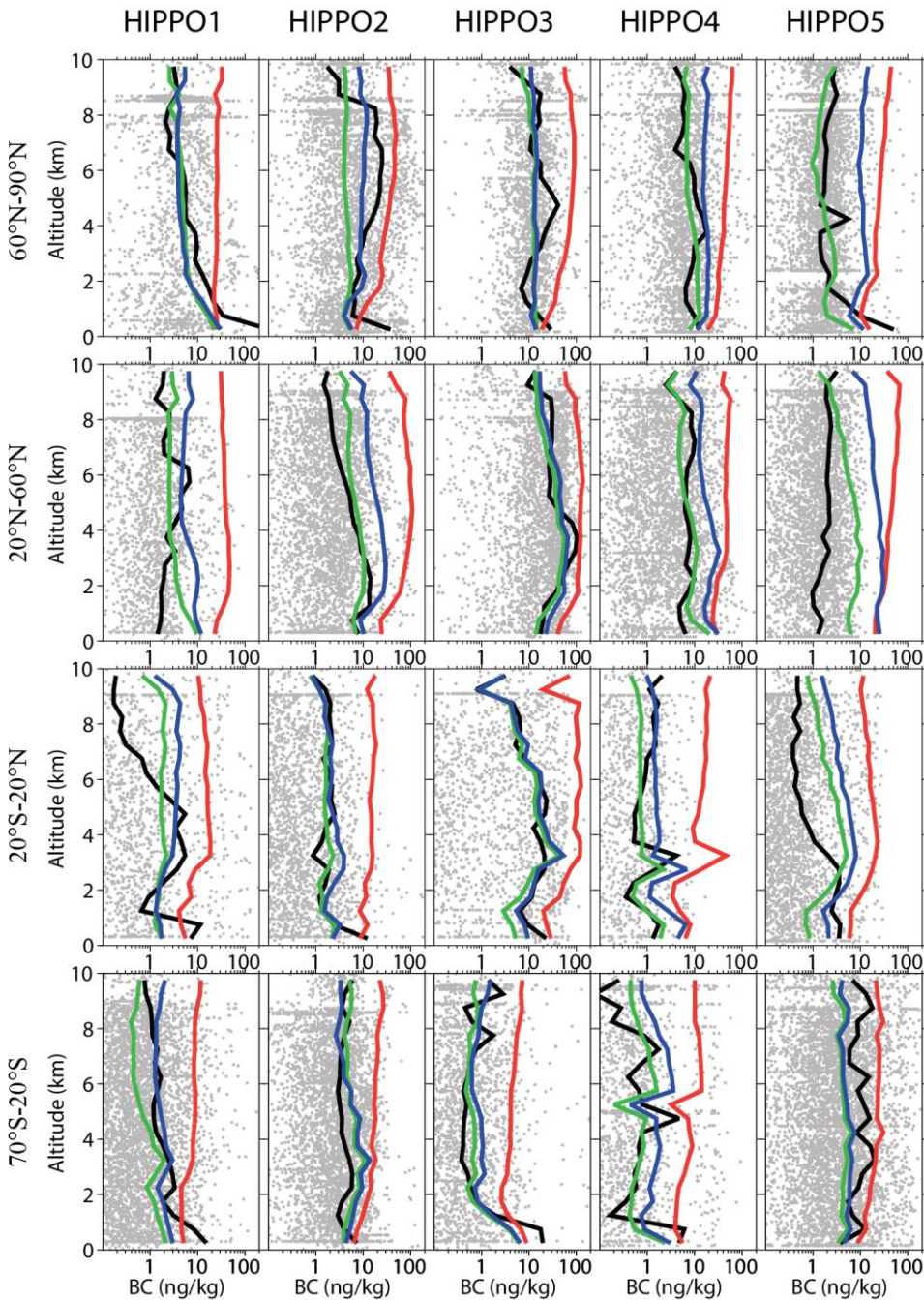


Figure S1. Vertical profiles of simulated and observed BC mass mixing ratios over 0.5 km altitude bins along the flight tracks of HIPPO 1-5 over the central Pacific Ocean (130°W-160°E). Data are shown separately as averaged over 70°S-20°S, 20°S-20°N, 20°N-60°N, and 60°N-90°N. The black, red, green, and blue lines are mean values of BC mixing ratios from observations,

default model, improved model with optimized region-specific aging timescale, and improved model using OH-dependent aging scheme respectively. The gray dots represent measured BC concentrations.

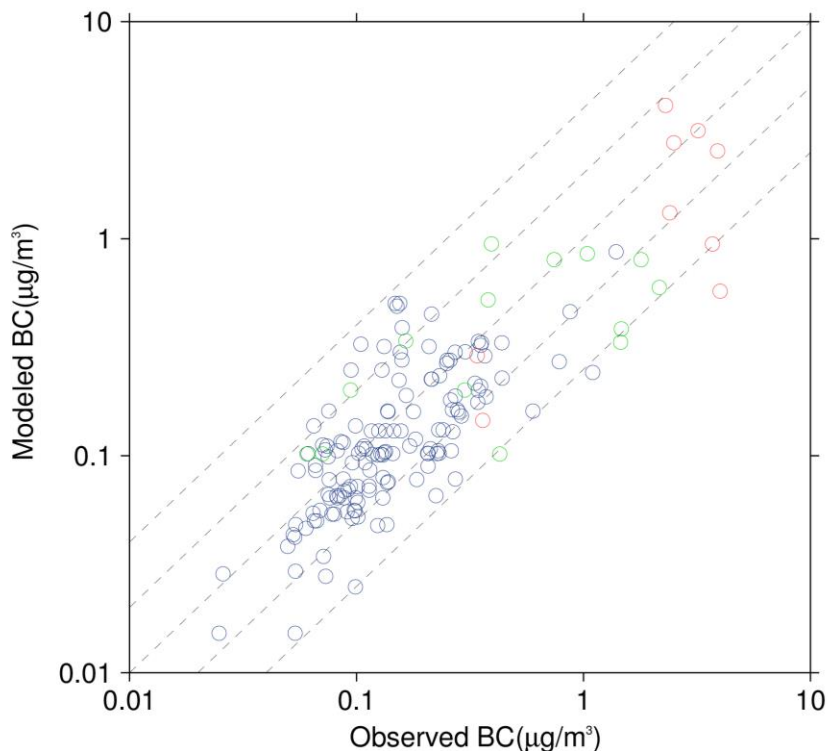


Figure S2. Modeled (employing OH-dependent aging scheme) versus observed surface annual mean concentration of BC at sites in IMPROVE (blue), EMEP (green), and China (red). Dash lines are 1 : 4, 1 : 2, 1 : 1, 2 : 1, and 4 : 1 ratio lines. BC observations in China are attained from Zhang et al. (2008).

Specific comments:

1. Page 16946 line 22-24: How fast is the aging rate so that the lifetime of BC is dominated by factors that control its local deposition?

Good question. In the model, hydrophobic BC cannot be removed by precipitation, while aging enables hydrophobic BC to convert to hydrophilic BC, and be removed by precipitation.

Therefore, when aging is slow, most BC stays hydrophobic near its source, and is not affected significantly by local precipitation. On the contrary, when aging is fast, BC is more susceptible to local precipitation, and might be removed shortly after emitted. To make this sentence clearer, we revise this sentence in abstract:

*“The lifetime of BC is more determined by factors that control local deposition rates (e.g. precipitation) when aging is fast versus slow.”*

2. Page 16946 line 27 – page 16947 line 1: This sentence repeats the first sentence of abstract. We revised this sentence in the abstract:

*“Our findings suggest that the aging timescale of BC varies significantly by region and season, and can strongly influence the contribution of source regions to BC burdens around the globe. Therefore, improving parameterizations of the aging process for BC is important for enhancing the predictive skill of global models. ”*

3. Page 16949 line 4: How thick must coating be for a hydrophobic BC to be named as a hydrophilic BC?

Kuwata et al (2009) estimate the critical condensed mass for hydrophobic BC converting to hydrophilic is 0.18 fg (supersaturation = 0.9%) and 0.07 fg (supersaturation = 1.3%) for 100-nm particles. Their results are based on their measurements in Tokyo, where they found the compounds of coating are mainly organic compounds. Besides thickness of coating, solubility of of the coating material is another important factor. Thus, the thickness of coatings to convert hydrophobic BC into hydrophilic BC may depend on the components of coatings as well as supersaturation.

4. Page 16954 line 20: It may be good to clarify the terms of “aging”, “aging rate”, and “aging timescale” used in the paper.

Good suggestion. We clarified the definitions of aging timescales and rate in the revised Introduction. Please see our revisions in the fourth paragraph of Section 1 or below:

*“...Exponential timescale for this aging process to occur, the so-called “aging timescale”, which is the reciprocal of aging rate, therefore highly influences the timing of cloud formation and wet deposition, and thus is of great research interest (Liu et al., 2011)...”*

We also clarified the definitions of aging in Section 2.4:

*“...Note that while we define aging timescale as that for converting BC from hydrophobic to hydrophilic, some other studies use this term to describe the change from thinly to thickly coated BC (Moteki et al., 2007;Saikawa et al., 2009).”*

5. Page 16954 line 25-28: Why does biomass burning BC have a larger fraction of coated particles and thicker coatings than urban BC? This seems to conflict with the discussion in section 2.1 (page 16949 line 14-24) that indicates that urban pollutions (i.e. sulfate, nitrate, ozone, and nitrogen oxide) are primary components in coating. Also the short aging timescale of East Asia BC summarized by the authors seems to not support this statement either.

It is shown by observations that biomass burning BC has a larger fraction of coated particles and

thicker coatings than urban BC as emitted (Schwarz et al., 2008). However, both thickness and solubility of coatings determine whether BC-containing particles can become cloud condensation nuclei (CCN). Thus, BC needs to be coated by sufficient soluble compounds (e.g. sulfate, nitrate, or organics), so as to be converted to CCN. Despite that previous studies find that biomass burning BC has a larger fraction of coated particles and thicker coatings, the solubility of the coatings on biomass burning emitted BC could be low. On the other hand, although coatings of urban BC are thinner, they could be sulfate or nitrate, which are extremely soluble (Johnson et al., 2005; Cheng et al., 2012). Future observations on the evolution of hygroscopicity of BC-containing particles from different source regions are needed. In the revised manuscript, we modified the paragraph in Section 3 to make it clearer:

*“Optimized aging timescales for each source region and season are shown in Table 1. Ranges of plausible values for each optimized aging timescale based on perturbation simulations are also summarized in Table S1 in the supplementary materials. As shown in Table 1, values differ significantly by source region and season. The aging timescale of BC from East Asia, North America, India, and Southeast Asia is in most cases relatively short (i.e., less than half a day). The optimized BC timescales reported here for East Asia and North America are consistent with observations in these regions, which show that BC is quickly mixed with hydrophilic species. For instance, observations over an urban region of Japan find that the timescale for BC to become internally mixed is 12 hours, with coatings made of primarily sulfate and soluble organic carbon (Moteki et al., 2007). In Beijing and Mexico City, urban BC is observed to become internally mixed with sulfate in a few hours (Johnson et al., 2005; Cheng et al., 2012). Over Southeast Asia, BC emissions are mainly anthropogenic in origin (with a fast aging rate), except during spring when large-scale biomass burning activities generate tremendous amounts of BC. The optimized springtime BC aging timescale for Southeast Asia is around 2 days, consistent with the findings of Shen et al. (2014). On the contrary, the optimized aging rate is relatively slow in the high-latitude regions (Canada, the former Soviet Union and in particular Europe) in all seasons except summer (June-July-August, JJA), which can be explained by slower photochemistry in high latitudes under low sunlight in non-summer months. Since measurements on BC aging timescale are scarce and limited to few places, more observations are needed to measure the hygroscopicity of BC-containing particles in different continents covering both source and downwind areas.”*

6. Page 16955 equation 3: How about longitude bins?

We mainly focus on the central Pacific (160 °E -130 °W), where BC is mostly contributed by long-range transport. So we average our results over this longitude band. The longitude range is described in section 2.3:

*“...Note that we use only the HIPPO observations taken in the Central Pacific Ocean (160 °E -130 °W) and ignore observations near source regions...”*

7. Page 16956 line 27 and Page 16957 line 1-2: Why is the aging of these urban polluted regions vary fast? Is it faster than that of biomass burning dominated regions such as South America,

Africa? I am confused since it is not consistent with the observation facts discussed in section 2.5 (see specific comments 5 above).

Thanks for bringing this question up. As we described in comment 5, though biomass burning BC may be more thickly coated comparing to what has been seen in urban regions, the solubility of coating materials between these two types of BC could be different. In the revised manuscript, we rewrote this paragraph in a clearer way. Please see the text below or our detailed response to comment 5.

*“Optimized aging timescales for each source region and season are shown in Table 1. Ranges of plausible values for each optimized aging timescale based on perturbation simulations are also summarized in Table S1 in the supplementary materials. As shown in Table 1, values differ significantly by source region and season. The aging timescale of BC from East Asia, North America, India, and Southeast Asia is in most cases relatively short (i.e., less than half a day). The optimized BC timescales reported here for East Asia and North America are consistent with observations in these regions, which show that BC is quickly mixed with hydrophilic species. For instance, observations over an urban region of Japan find that the timescale for BC to become internally mixed is 12 hours, with coatings made of primarily sulfate and soluble organic carbon (Moteiki et al., 2007). In Beijing and Mexico City, urban BC is observed to become internally mixed with sulfate in a few hours (Johnson et al., 2005; Cheng et al., 2012). Over Southeast Asia, BC emissions are mainly anthropogenic in origin (with a fast aging rate), except during spring when large-scale biomass burning activities generate tremendous amounts of BC. The optimized springtime BC aging timescale for Southeast Asia is around 2 days, consistent with the findings of Shen et al. (2014). On the contrary, the optimized aging rate is relatively slow in the high-latitude regions (Canada, the former Soviet Union and in particular Europe) in all seasons except summer (June-July-August, JJA), which can be explained by slower photochemistry in high latitudes under low sunlight in non-summer months. Since measurements on BC aging timescale are scarce and limited to few places, more observations are needed to measure the hygroscopicity of BC-containing particles in different continents covering both source and downwind areas.”*

8. Page 16958 line 12-14: How sensitive is the summarized BC aging timescale to a change in precipitation? In other words, what is the potential uncertainty of aging timescale in response to a potential bias in precipitation predicted by MOZART-4?

Good question. MOZART-4 is driven by reanalysis meteorology, and precipitation was found to have a better agreement with observations when water vapor concentrations was calculated online (the preferred mode of operation in MOZART-4, see Emmons et al., 2010). As shown in Figure S4 (see below), the pattern of precipitation in MOZART-4 is in general consistent with NCEP reanalysis, with moderate difference in magnitude.



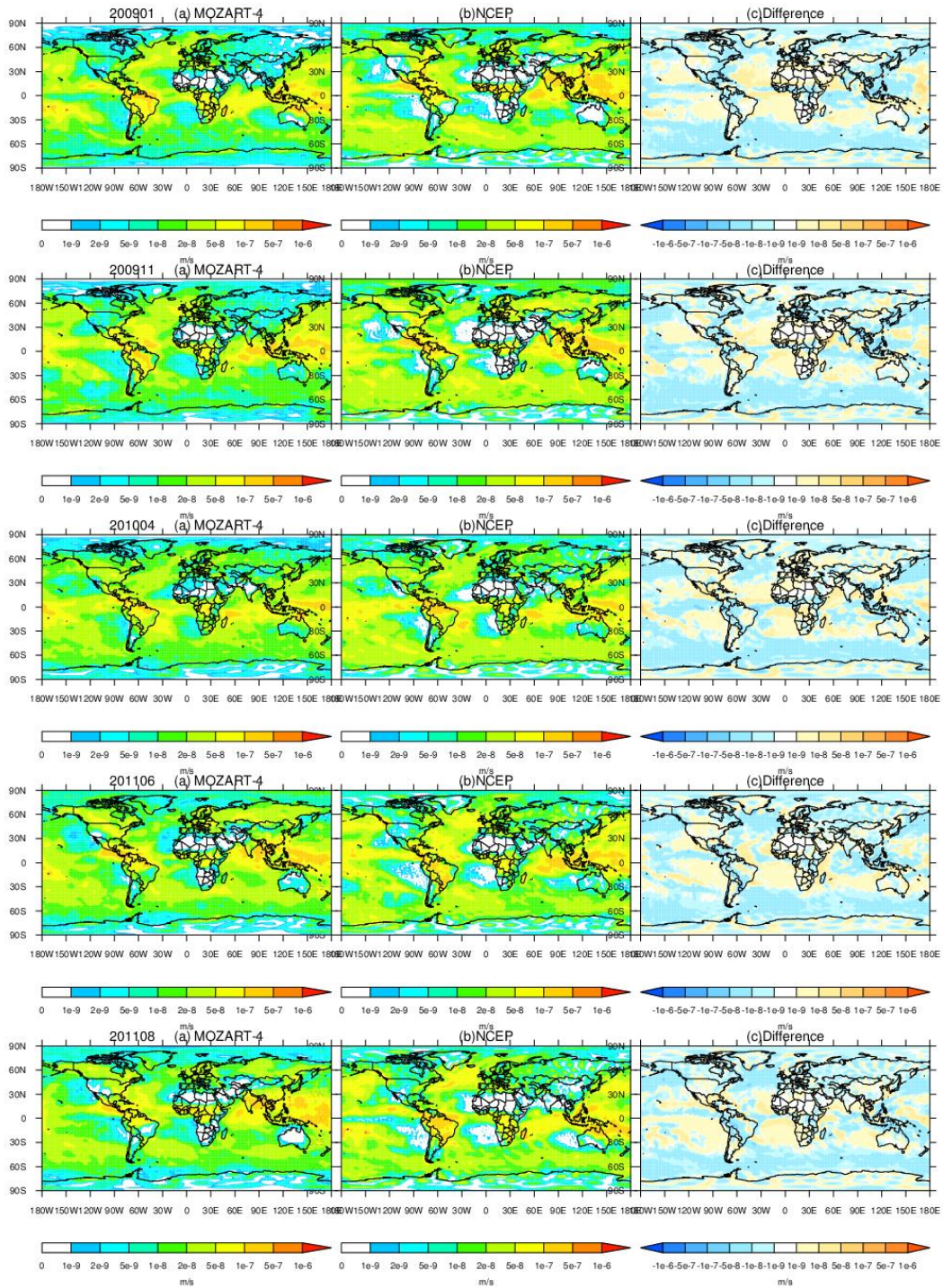


Figure S4. Average precipitation of MOZART-4 model, NCEP reanalysis meteorology, and their difference (MOZART-4 minus NCEP) during HIPPO I (January, 2009), HIPPO II (November, 2009), HIPPO III (April, 2010), HIPPO IV (June, 2011), and HIPPO V (August, 2011).

On the other hand, we agree with the reviewer that bias in precipitation might also influence our results of optimization. According to our wet deposition scheme (see Equation 2), wet removal of BC increases as precipitation increases if cloud water content keeps the same. So the change in precipitation will influence the loadings of BC over the Pacific Ocean and other regions as well. We added discussion on the uncertainties related to precipitation in Caveat Section:

*“...Firstly, we assume that model parameterizations of wet and dry deposition, precipitation, transport, and emissions are realistic, even though these processes also affect BC distributions and have uncertainties (Vignati et al., 2010; Fan et al., 2012). Consequently, the optimized aging timescales may partially counter biases in these processes (i.e. other than aging), and may vary according to the model used. For example, as model resolution increases, aerosol-cloud interactions in climate models can be better resolved, which can improve the simulation of BC transport (Ma et al., 2013; Ma et al., 2014). Therefore, the optimized aging timescales might change if models with different cloud schemes or spatial resolutions are used...”*

We also revised the explanations for the remaining bias in section 3:

*“In a few cases, relatively large differences between the improved model and observations remain. These differences could be attributed to any number of factors (e.g., emissions, transport, cloud/precipitation, aging process, wet removal efficiency, etc.). For example, models could misrepresent BC wet deposition, originating from biases in precipitation. As shown in Figures S4 in the supplementary materials, though MOZART-4 generally captures well the spatial extent of precipitation during all HIPPO campaigns, biases occasionally appear when comparing to the NCEP reanalysis over the western Pacific...”*

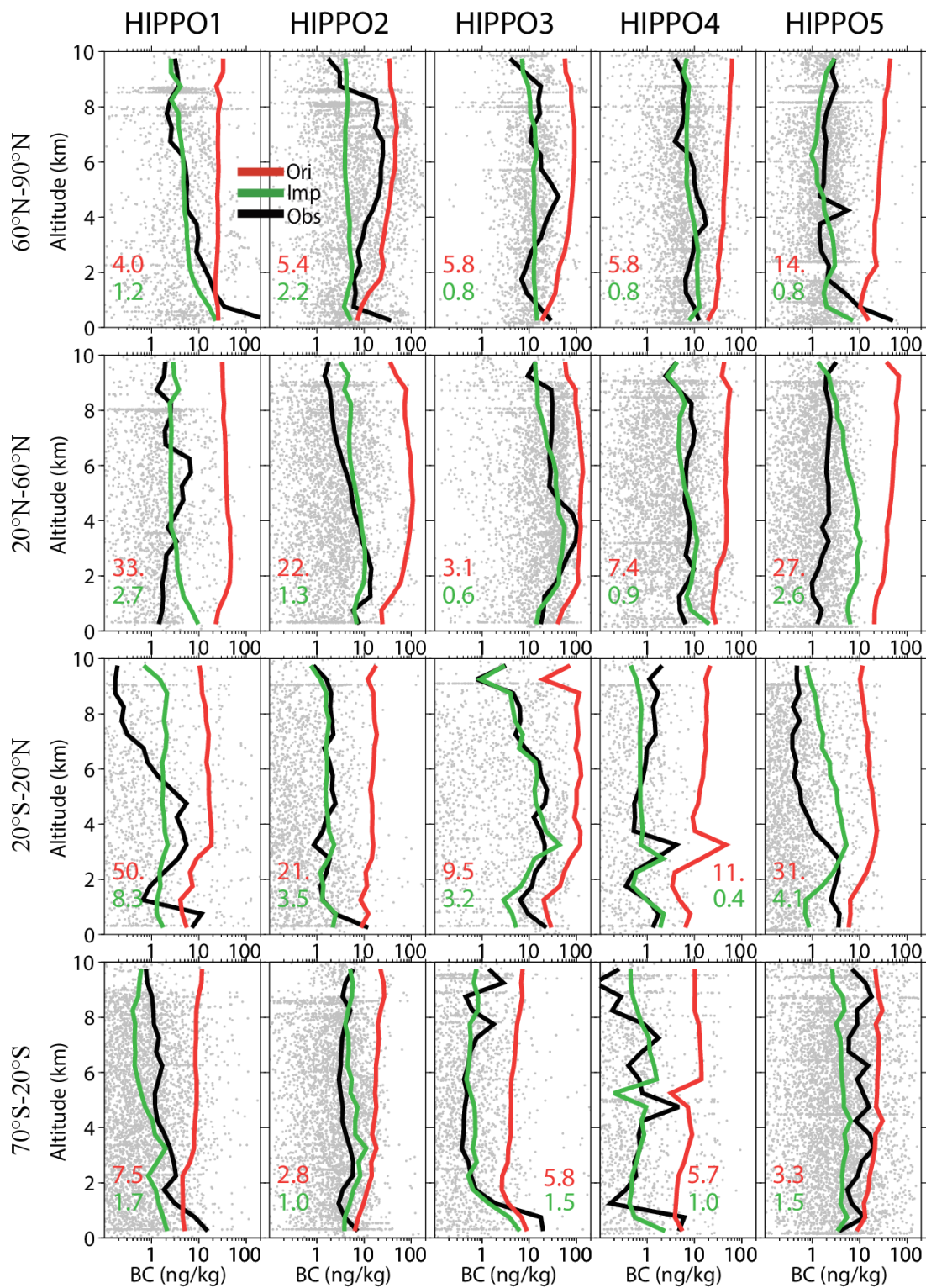
9. Figure 5: It is interesting to know that Africa emission is not a dominant contributor to most of the Pacific Ocean since it is the largest contributor to global BC (Page 16960 line 10-11) and Africa is closest to the Pacific Ocean.

Although Africa is the largest contributor to global BC, due to wind directions and the long distance of Africa to the Pacific Ocean, Africa is not the largest contributor to the Pacific Ocean. On the other hand, as shown in Figure 5, Africa contributes the most to some areas in the Atlantic Ocean and the Indian Ocean. In the future, measurements over the Atlantic Ocean and Indian Ocean can be very helpful to clarify the contribution of African BC to the Pacific.


Technique corrections: 1. Figure 4: Please change color of improved model results (green line and number) so that it is more distinct from the grey dots that represent measured BC concentrations.

Thanks for this correction. We have changed the color, format, and position of dots and numbers to make them more readable in Figure 4, as shown below:





## References

- Cheng, Y. F., Su, H., Rose, D., Gunthe, S. S., Berghof, M., Wehner, B., Achtert, P., Nowak, A., Takegawa, N., Kondo, Y., Shiraiwa, M., Gong, Y. G., Shao, M., Hu, M., Zhu, T., Zhang, Y. H., Carmichael, G. R., Wiedensohler, A., Andreae, M. O., and Poschl, U.: Size-resolved measurement of the mixing state of soot in the megacity Beijing, China: diurnal cycle, aging and parameterization, *Atmospheric Chemistry and Physics*, 12, 4477-4491, DOI 10.5194/acp-12-4477-2012, 2012.
- Johnson, K. S., Zuberi, B., Molina, L. T., Molina, M. J., Iedema, M. J., Cowin, J. P., Gaspar, D. J., Wang, C., and Laskin, A.: Processing of soot in an urban environment: case study from the Mexico City Metropolitan Area, *Atmospheric Chemistry and Physics*, 5, 3033-3043, 2005.
- Kuwata, M., Kondo, Y., and Takegawa, N.: Critical condensed mass for activation of black carbon as cloud condensation nuclei in Tokyo, *Journal of Geophysical Research-Atmospheres*, 114, Artn D20202 10.1029/2009jd012086, 2009.
- Schwarz, J. P., Gao, R. S., Spackman, J. R., Watts, L. A., Thomson, D. S., Fahey, D. W., Ryerson, T. B., Peischl, J., Holloway, J. S., Trainer, M., Frost, G. J., Baynard, T., Lack, D. A., de Gouw, J. A., Warneke, C., and Del Negro, L. A.: Measurement of the mixing state, mass, and optical size of individual black carbon particles in urban and biomass burning emissions, *Geophysical Research Letters*, 35, Artn L13810 Doi 10.1029/2008gl033968, 2008.
- Zhang, X. Y., Wang, Y. Q., Zhang, X. C., Guo, W., and Gong, S. L.: Carbonaceous aerosol composition over various regions of China during 2006, *Journal of Geophysical Research-Atmospheres*, 113, Artn D14111 Doi 10.1029/2007jd009525, 2008.
- 

## Response to Anonymous Referee #2

(Note: Reviewer comments are listed in grey, and responses to reviewer comments are in black. Pasted text from the new version of the paper is in italics.)

This paper presents a global modeling analysis to constrain the first-order aging timescale of black carbon based on observations from the HIPPO campaign. The analysis involves performing several sensitivity studies where the aging time scale was varied, with the BC tracer tagged according to different geographic source regions. Optimal aging time scales for each source region are then found by minimizing the error between simulated BC mixing ratios and HIPPO observations. The tagging of BC also allows quantifying the contribution of BC from different source regions to various receptor regions, including the Pacific Ocean, which is an area of interest as BC over this area is suspected to have significant climate impacts.

This is an interesting paper, which makes innovative use of HIPPO data. It supports previous studies that found that the first-order aging time scale that is used in many global models should not be a fixed value, but should depend on local conditions.

The paper fits well into the scope of ACP and is for the most part well-written. The discussion in Section 5 is very instructive. My main comments concern the optimization procedure in Section 2.5. I hope the reviewers can resolve these in a revised version.

We greatly appreciate the reviewer's thorough and constructive review. We believe revising the paper according to the reviewer's comments has considerably improved the paper. We have merged all of the suggestions into the revised manuscript. Please see our response to each comment below:

Major Comments:

The description of the optimization procedure in Section 2.5 needs to be improved (line 22 – 25). It sounds like the authors performed 13 simulations, with constant aging time scale for each of these simulations. It is not clear how the area-specific aging time scales are obtained from these 13 simulations. I believe that the constraint is used that  $BC(i; j; t) = \sum_{k=1}^{n_{source}} P_{source k} BC(i; j; t; k)$ , and then  $BC(i; j; t)$  is reconstructed using all possible recombinations of  $BC(i; j; t; k)$  from the 13 sensitivity runs. Finally, it is checked which  $BC(i; j; t)$  best matches the observations. Please clarify this procedure.

Thanks for this great suggestion. The reviewer's description is correct. We have clarified the description of the optimization procedure following the reviewer's suggestion. Please see our revisions in Section 2.5 in the revised manuscript or below:

*“We perform 13 simulations, each with different constant aging timescales (i.e. 4, 8, 12, 18, 24, 27.6, 38.4, 48, 60, 90, 120, 160 or 200 hours). Every simulation tags BC from each of 13 regions (i.e., North America, East Asia, Canada, ...); as mentioned in Section 2.3,*

$BC_m(j,k)=\sum_r BC_m(j,k,r)$ , where  $r$  denotes each region. We construct  $BC_m(j,k)$  using all possible combinations of  $BC_m(j,k,r)$  from the 13 simulations. Then we check which combination of  $BC_m(j,k,r)$  best matches BC observations. Note that we constrain the aging rates of BC emitted from Africa, South America, and Australia to be the same since these three regions are all biomass burning dominated sources in the Southern Hemisphere, which effectively reduces the total number of tagged tracers from 13 to 11. Thus, we determine the best-fit BC aging timescale for each source region (out of  $13^{11}$  combinations in total) that minimizes MNAE.”

If this is what happens, my main concern is how stable the procedure is, i. e., given the large number of permutations to calculate candidate  $BC(i; j; t)$  values, it could happen that many different combinations of  $BC(i; j; t; k)$  lead to a similarly small error, and that the authors are fitting noise. One way to check this would be to use a testing and a training set, which might not be possible given the limited amount of observations. Another way to check this would be to visually inspect plots where the error is graphed as a function of parameter that is varied, keeping all other parameters constant. It should be very obvious if these curves look sufficiently smooth so that a robust minimum can be identified. The values listed in Table 2 do look questionable: two thirds of these values are either 4 or 200, which are the minimum and maximum values in the set of aging time scales used for the sensitivity runs. This could mean that the range of aging time scales chosen was not large enough. The authors discuss the physical interpretation of the optimized aging time scales on page 16957, but there are several examples that are hard to interpret. For example, for SU the time scale is 200 h for June and 4 h for August. Several other examples along this line can be found.

Excellent point. Following the reviewer’s suggestion, we checked the sensitivity of the summed error to aging timescale changes. Specifically, we varied aging timescale in each region while keeping the aging timescale of other regions as previously optimized. We plotted the error versus the varied aging timescales for different regions, and added Figure S5 in the supplementary material:

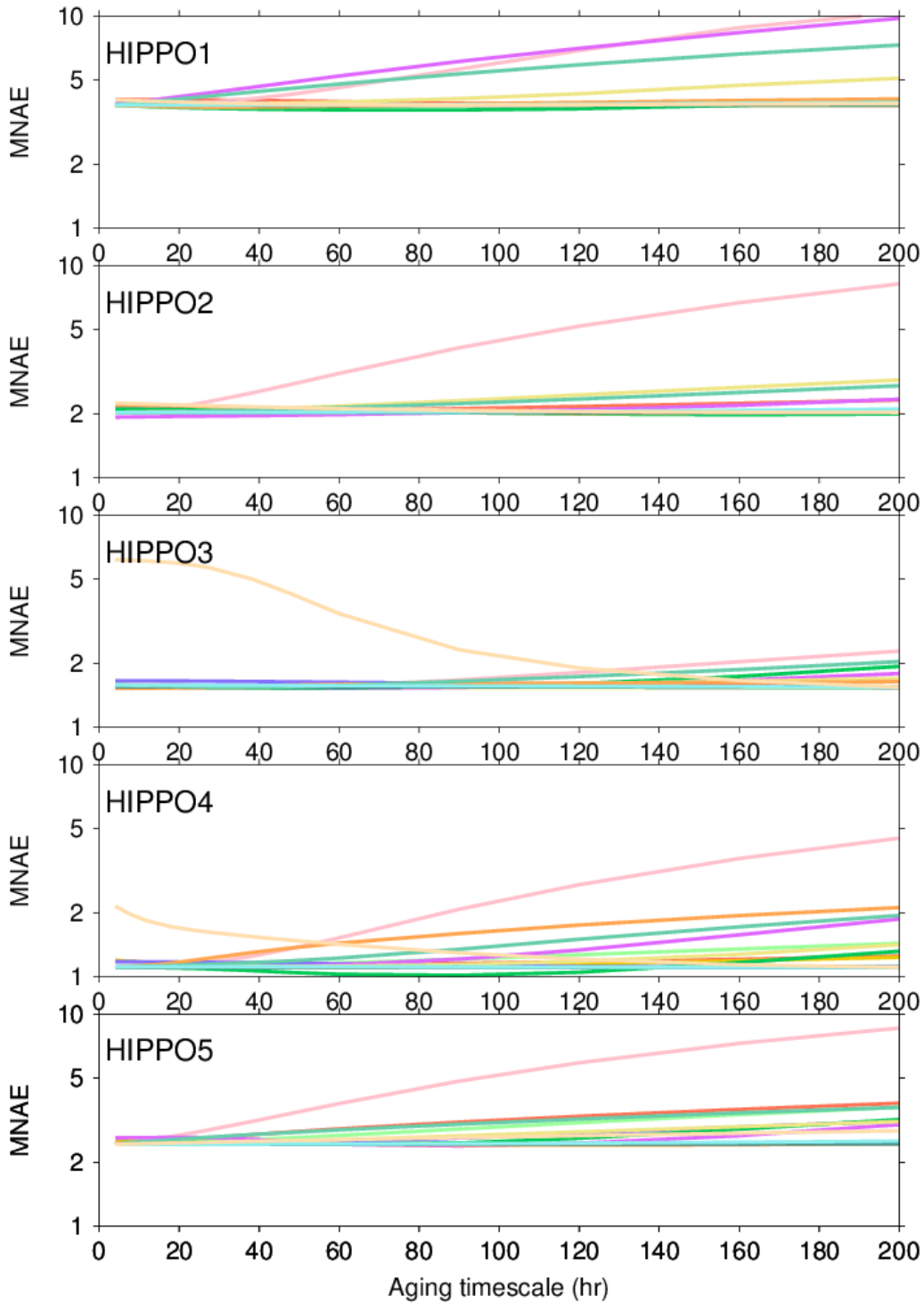


Figure S5.

Mean normalized absolute error (MNAE) as a function of varying aging timescale for each region while keeping the aging timescale of other regions as optimized. Different colors denote 13 regions.



As shown in Figure S5, all curves are smooth. For some regions, it is easy to identify a robust minimum, while for some other regions the sensitivity of MNAE to aging timescale change is small. Therefore, our optimization on BC aging may be more robust to regions with significant contributions to BC burdens than insignificant contributors. The difference in sensitivity of MNAE on aging timescales in different regions inspires us to estimate the potential range of our results based on the information in Figure S5. For each HIPPO campaign, we assign a range of BC aging timescales for a region if the corresponding MNAE value is no larger than that of the optimized MNAE plus a small perturbation  $\Delta E$ . A narrow range may indicate that this optimized aging timescale is more robust than that with a broader range. Table S1 in the supplementary material (or below) illustrates the ranges for each optimized aging timescale when 0.01 is used for  $\Delta E$ . We found that our optimized aging timescales are more robust for specific regional BC tracers (e.g. EA, IN, etc.) than others (e.g. MA, SA, etc.).

Table S1. Range of plausible aging timescales (units = hours) for 13 regions (For each HIPPO campaign, we assign a range of BC aging timescales for a region if the corresponding MNAE value is no larger than that of the optimized MNAE plus a small perturbation  $\Delta E=0.01$ ).

		CA	SU	EU	MA	EA	ME	NA	SE	IN	AF	SA	AU	RR
<b>HIPPO1</b>	Jan	12-200	4-200	90-120	4-200	4-8	4-60	160-200	4-4	4-8	4-4	4-160	4-60	90-120
<b>HIPPO2</b>	Nov	90-200	4-200	120-160	4-200	4-4	4-60	4-24	4-8	4-8	4-90	90-200	90-160	160-200
<b>HIPPO3</b>	Apr	4-200	60-200	200-200	4-200	38. 4-48	160-200	4-60	27. 6-48	4-48	18-90	18-60	4-27. 6	200-200
<b>HIPPO4</b>	Jun	38. 4-90	4-18	120-200	4-200	4-8	4-200	4-18	4-8	4-48	4-38. 4	4-120	4-8	200-200
<b>HIPPO5</b>	Aug	90-120	4-4	4-38. 4	4-120	4-4	4-60	4-4	4-4	4-12	60-90	60-60	48-160	4-4

In the revised manuscript, we also include the following discussion on the uncertainties in optimized aging timescales in Section 6:

*“...Fourthly, the computed optimized aging rate is more accurate for tracers (i.e. source regions) with larger emissions and in closer proximity to the Pacific Ocean (e.g. East Asia). This is because modeled BC concentrations over the Pacific (i.e. the location of HIPPO observations) for each latitude and longitude bin are typically dominated by only a few source regions, and the sensitivity of MNAE on each regional BC tracer is different (see Figure S5 in the supplementary material). For some source regions, observations in other remote regions would provide a better constraint for optimizing aging timescale in the model. More specifically, aircraft observations over the Atlantic Ocean could better constrain aging timescales for BC emitted from Africa and South America. As new observations become available, this study could be repeated to more accurately optimize the aging timescale for source regions with lower relative contributions to BC over the Pacific (e.g. Middle Asia)...”*

We also agree with the reviewer that our approach do have limitations and the optimized results may partially depend on performance of modeling processes beyond aging. In addition, this study only used 13 choices of aging timescales for regions, which cannot cover all the possibilities happening in the real atmosphere. Thus, every given number may actually represent a range. For example, ‘4h’ and ‘200h’ in Table 1 can mean ‘less than 8h’(or fast aging) and ‘greater than 160 hours’ (or slow aging), respectively. Nevertheless, the goal of our aging optimization is not to

provide a set of accurate aging timescales that can be directly used in models, but to utilize every HIPPO observation at most to inform the possible spatiotemporal pattern of aging timescales globally. Our results may indicate that the aging rate of BC may change by region and season, as opposed to a fixed aging timescale currently widely used in many chemical transport models. In addition, we extensively expanded the caveats on Section 6 to address the uncertainties of our approach:

*“We note that there are multiple limitations to our approach. Firstly, we assume that model parameterizations of wet and dry deposition, precipitation, transport, and emissions are realistic, even though these processes also affect BC distributions and have uncertainties (Vignati et al., 2010; Fan et al., 2012). Consequently, the optimized aging timescales may partially counter biases in these processes (i.e. other than aging), and may vary according to the model used. For example, as model resolution increases, aerosol-cloud interactions in climate models can be better resolved, which can improve the simulation of BC transport (Ma et al., 2013; Ma et al., 2014). Therefore, the optimized aging timescales might change if models with different cloud schemes or spatial resolutions are used. Secondly, due to limitations in computing resources, we carry out simulations assuming 13 discrete values for aging timescale. Optimized aging timescale could have been more precisely determined with more simulations. Thirdly, the optimized aging results may somewhat depend on the error matrix chosen. We conduct additional simulations with different error matrices (see Table S2, S3 in supplementary material). The results are overall similar, but in some cases moderate differences are found. Fourthly, the computed optimized aging rate is more accurate for tracers (i.e. source regions) with larger emissions and in closer proximity to the Pacific Ocean (e.g. East Asia). This is because modeled BC concentrations over the Pacific (i.e. the location of HIPPO observations) for each latitude and longitude bin are typically dominated by only a few source regions, and the sensitivity of MNAE on each regional BC tracer is different (see Figure S5 in the supplementary material). For some source regions, observations in other remote regions would provide a better constraint for optimizing aging timescale in the model. More specifically, aircraft observations over the Atlantic Ocean could better constrain aging timescales for BC emitted from Africa and South America. As new observations become available, this study could be repeated to more accurately optimize the aging timescale for source regions with lower relative contributions to BC over the Pacific (e.g. Middle Asia). The goal of the optimization presented here is not to provide precise aging timescales that can be directly used in models, since models differ significantly in their parameterizations of physical and chemical processes, particularly the wet scavenging. Also, BC aging includes complicated chemistry and physics, but is simplified in our modeling as a first-order conversion from hydrophobic to hydrophilic BC. Nevertheless, this study proposes a useful method to utilize all HIPPO observations and explore the spatiotemporal pattern of BC aging timescales globally.”*

Minor comments:

1. Rearrange the order of the columns in table 1 and 2, so that they show the source regions in the same order, to facilitate the comparison of the two tables for the reader.

Thanks for pointing out this mistake. We have changed the order of the columns in Table 2 to make it consistent with other tables.

2. Section 2.2: How do you know that using the updated dry and wet deposition schemes results in an improvement of the model performance?

Good question. First, the original model treats these processes in simplified, and to some extent arbitrary ways. The first order wet scavenging rate for BC is set to 20% of that for nitric acid, and dry deposition velocity of BC is fixed at  $0.1 \text{ cm s}^{-1}$  everywhere (Emmons et al., 2010). On the contrary, our employed deposition schemes are more physically or experimentally based, and have been shown to work well in other similar models by previous studies (Liu et al., 2011; Wang et al., 2011; Hodnebrog et al., 2014). Second, after implementing these schemes in MOZART-4, we also evaluated the model and found that MNAE is at least reduced by a factor of 2, if compared to the original model.

3. p. 16953, line 27: “approximately equal”: Please quantify this statement.

We quantified the relative difference between the sum of tagged BC and untagged BC at the surface and at 500hPa. The relative difference is in most cases less than 1% with the largest bias less than 4%.

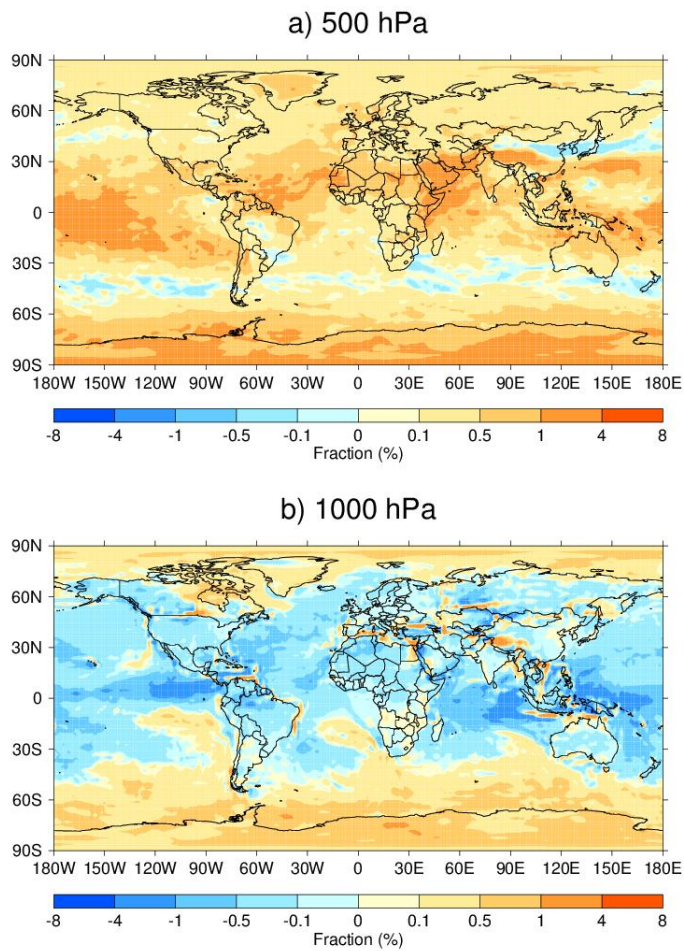


Figure R1. The relative difference between the sum of tagged BC and untagged BC a) at 500hPa and b) at 1000 hPa.

We follow the reviewer’s suggestion and quantitatively described the difference in the revised manuscript (see below):

*“The relative difference between the sum of the 13 regional BC tracers and the untagged BC is small (i.e., in most cases less than 1% with the largest biases less than 4%). Therefore, the sum of the 13 regional BC tracers is approximately equal to the untagged BC.”*

4. “Normalized mean absolute error” should be “Mean normalized absolute error”

Thanks for correcting this. We have corrected all the uses of this term in the paper. Now we use Mean normalized absolute error (MNAE).

5. In equation (3), are the simulated and observed BC values taken at the same time?

We compared the daily model output to the HIPPO observational data. We have clarified this issue in the revised manuscript in Section 2.5:

*“The model output daily averaged BC mixing ratios. For every record in HIPPO data (averaged in every 10s), we find modeled BC mixing ratio at the same longitude, latitude, altitude, and on the same day correspondingly. In this way, modeled and observed BC mixing ratios are paired, and then are averaged respectively over latitude and altitude bins.”*



### Response to Anonymous Referee #3

(Note: Reviewer comments are listed in grey, and responses to reviewer comments are in black. Pasted text from the new version of the paper is in italics.)

The study Zhang et al., “Long range transport of black carbon to the Pacific Ocean and its dependence on aging timescale”, used a chemical transport model (MOZART-4) to test the sensitivity of BC simulations to prescribed aging timescales. The authors tagged the emission sources to study source-receptor relationships. They also used observations to calibrate the aging timescale parameters, and discussed the difference between the default and the improved model. Overall I find this study interesting and scientifically important. The manuscript is well-prepared that it is straightforward to follow and concise. Therefore, I recommend the paper to be published on ACP. I only have a few minor comments for the authors to consider if they think they can further improve the paper:

We thank the helpful comments and suggestions indicated by the reviewer. We believe addressing his suggestions greatly improve the quality of our paper. Please see our response to each comment below.

1. Page 16950, line 22: The citation Emmons et al., 2010 should be placed right after MOZART-4, instead of after NCAR.

Thanks for correcting this. We have revised the sentence as the follow:

*“In this research, we use the Model for Ozone and Related Chemical Tracers, version 4 (MOZART-4) (Emmons et al., 2010), a global chemical transport model developed at the National Center for Atmospheric Research (NCAR). ”*

2. Page 16950, line 24: Please provide the citation for MATCH.

Thanks for pointing this out. We added the following citation in the revised manuscript (see Section 2.1).

*“Built on the framework of the Model of Atmospheric Chemistry and Transport (MATCH) (Rasch et al., 1997) with a series of updates...”*

*Full citation:*

*Rasch, P. J., Mahowald, N. M., and Eaton, B. E.: Representations of transport, convection, and the hydrologic cycle in chemical transport models: Implications for the modeling of short-lived and soluble species, Journal of Geophysical Research-Atmospheres, 102, 28127-28138, Doi 10.1029/97jd02087, 1997.*

3. Page 16951, line 13: This model is run at rather coarse resolution. I wonder if the conclusion will change with higher model resolution. It might be interesting to cite a few papers and a few sentences to acknowledge changing model resolutions might affect aerosol-cloud interactions, and change the sensitivity test of aging timescale here.

Thanks for bringing up this important issue. We agree with the reviewer that changing resolution in climate models might change the optimized aging timescales. We have added discussions and cited more papers on resolution and aerosol-cloud interactions in the Caveat section:

*“For example, as model resolution increases, aerosol-cloud interactions in climate models can be better resolved, which can improve the simulation of BC transport (Ma et al., 2013;Ma et al., 2014). Therefore, the optimized aging timescales might change if models with different cloud schemes or spatial resolutions are used.”*

*Citations:*

*Ma, P. L., Rasch, P. J., Fast, J. D., Easter, R. C., Gustafson, W. I., Liu, X., Ghan, S. J., and Singh, B.: Assessing the CAM5 physics suite in the WRF-Chem model: implementation, resolution sensitivity, and a first evaluation for a regional case study, Geosci. Model Dev., 7, 755-778, 10.5194/gmd-7-755-2014, 2014.*

*Ma, P. L., Rasch, P. J., Wang, H. L., Zhang, K., Easter, R. C., Tilmes, S., Fast, J. D., Liu, X. H., Yoon, J. H., and Lamarque, J. F.: The role of circulation features on black carbon transport into the Arctic in the Community Atmosphere Model version 5 (CAM5), Journal of Geophysical Research-Atmospheres, 118, 4657-4669, 10.1002/jgrd.50411, 2013.*

4. Page 16951, line 16: I am confused. Is MACCity emissions used for IPCC-AR5 simulations? What about the Lamarque et al. (2010) emissions?

Thanks for catching this mistake. According to the website [http://accent.aero.jussieu.fr/MACC\\_metadata.php](http://accent.aero.jussieu.fr/MACC_metadata.php), the suggested documentation should be Lamarque et al., ACP, 2010. Also, “In support of the fifth IPCC-AR5 (Intergovernmental Panel for Climate Change Assessment Report 5), the ACCMIP (Atmospheric Chemistry and Climate - Model Intercomparison Project) historical emissions dataset has been developed (Lamarque et al, 2010), on a decadal basis (from 1850 to 2000 for the historical dataset), as well as emissions scenarios called RCPs (Representation Concentration Pathways, Van Vuuren et al., 2010). As part of two projects funded by the European Commission, MACC and CityZen, the ACCMIP and the RCPs emissions dataset have been adapted and extended on a yearly basis for the period 1990-2010. For anthropogenic emissions, emission data were interpolated on a yearly basis between the base years 1990, 2000, 2005 and 2010. For the years 2005 and 2010, the RCP 8.5 emissions scenario was chosen (4 emissions scenarios were developed in support of the IPCC-AR5: RCP 2.6, RCP 4.5, RCP 6, RCP 8.5).For biomass burning emissions, the ACCMIP dataset was extended as well on a monthly basis. This 'extension' of the ACCMIP and RCPs emission dataset for the MACC and CityZEN projects is referred to as MACCity (MACC/CityZen) emission dataset.” We modified the sentence to make it more precise:

*“Anthropogenic emissions are based on the MACCity emission inventory (<http://www.pole-ether.fr/eccad>), which is extended from the database used for IPCC Coupled Model Intercomparison Project (Lamarque et al., 2010).”*

5. Page 16957, line 2: I think it might read better if you move the discussion from line 8 (mixing in Asia and North America is quick) to line 2, following “(less than half a day)”.

We took the reviewer’s suggestion and revised this paragraph as below:

*“Optimized aging timescales for each source region and season are shown in Table 1. Ranges of plausible values for each optimized aging timescale based on perturbation simulations are also summarized in Table S1 in the supplementary materials. As shown in Table 1, values differ significantly by source region and season. The aging timescale of BC from East Asia, North America, India, and Southeast Asia is in most cases relatively short (i.e., less than half a day). The optimized BC timescales reported here for East Asia and North America are consistent with observations in these regions, which show that BC is quickly mixed with hydrophilic species. For instance, observations over an urban region of Japan find that the timescale for BC to become internally mixed is 12 hours, with coatings made of primarily sulfate and soluble organic carbon (Moteki et al., 2007). In Beijing and Mexico City, urban BC is observed to become internally mixed with sulfate in a few hours (Johnson et al., 2005; Cheng et al., 2012). Over Southeast Asia, BC emissions are mainly anthropogenic in origin (with a fast aging rate), except during spring when large-scale biomass burning activities generate tremendous amounts of BC. The optimized springtime BC aging timescale for Southeast Asia is around 2 days, consistent with the findings of Shen et al. (2014). On the contrary, the optimized aging rate is relatively slow in the high-latitude regions (Canada, the former Soviet Union and in particular Europe) in all seasons except summer (June-July-August, JJA), which can be explained by slower photochemistry in high latitudes under low sunlight in non-summer months. Since measurements on BC aging timescale are scarce and limited to few places, more observations are needed to measure the hygroscopicity of BC-containing particles in different continents covering both source and downwind areas.*

*The seasonality of aging timescale reported here is largely consistent with Liu et al. (2011), who develop a parameterization for BC aging rate as a function of OH radical concentration. In this study, we further improve the parameterization of Liu et al. (2011) by finding best-fit values for constants that best match HIPPO observations with reference to our BC aging timescales. After conducting additional sensitivity simulations, we find that a set of parameters (i.e.,  $\beta=2.4 \times 10^{-11}$ , and  $\gamma=1 \times 10^{-6}$  in Equation (4) in Liu et al. (2011)) when employed in MOZART-4 can fit well the HIPPO observations as well as ground observations (see Figure S1 and S2 in supplementary material).”*

6. Regarding Figure 4, I notice that even with the improved model in many cases the model still under-estimate the BC concentration by an order of magnitude, but there is no discussion on this feature. Please elaborate.

In the revised manuscript, we further expanded the discussion on the differences between the modelled and observed BC concentrations. Please see the revised text in Section 3 or below:

*“In a few cases, relatively large differences between the improved model and observations remain. These differences could be attributed to any number of factors (e.g., emissions, transport, cloud/precipitation, aging process, wet removal efficiency, etc.). For example, models could misrepresent BC wet deposition, originating from biases in precipitation. As shown in Figures S4 in the supplementary materials, though MOZART-4 generally captures well the spatial extent of precipitation during all HIPPO campaigns,*

*biases occasionally appear when comparing to the NCEP reanalysis over the western Pacific. As another example, the model uses a monthly biomass burning emission inventory. This means that modeled emissions lack daily variation in biomass burning activities that could be important where biomass burning emissions dominate BC loading. Underestimates in BC mixing ratio may be partially due to abrupt emissions events that are not captured by the model. Lastly, since this study assumes that BC aging timescale in all the southern hemispheric continents is the same, we do not account for variability in BC aging rates from these regions that may exist in reality.”*

7. Page 16959, line 12: Since the term “Pacific Ocean” has been used many times previously in the text, the acronym “PO” is out of place and not needed.

We follow the reviewer’s suggestions and removed this acronym in the revised manuscript.

8. Page 16961, line 15: Perhaps replace “dT/dtau” with “S=dT/dtau”, and discuss S later in this paragraph.

9. Page 16962, line 1: Please elaborate why the theoretical value of the slope is 0.8.

Good suggestion. We have substituted dT/dtau by s in the revised manuscript.

9. Page 16962, line 1: Please elaborate why the theoretical value of the slope is 0.8.

According to equation 7, theoretically,  $s = \frac{(1-\alpha)K_w}{(K_D+K_w)(1+K_D\tau)^2}$ . If dry deposition coefficient ( $K_D$ ) is negligible, then  $s = 1 - \alpha$ .  $\alpha = 0.2$  in the model, so  $s = 0.8$ . We revised the text a bit to make it more understandable:

*“In MOZART-4,  $\alpha$  is assumed to be 0.2 for all emission sources. So if  $K_D$  is negligible, the theoretical slope of the T- $\tau$  curve is  $1-0.2=0.8$ , which is very close to the curve for untagged BC (black line) in Figure 6. “*

#### References:

- Cheng, S. F., Tom, K., and Pecht, M.: Failure Causes of a Polymer Resettable Circuit Protection Device, J Electron Mater, 41, 2419-2430, DOI 10.1007/s11664-012-2148-9, 2012.
- Emmons, L. K., Walters, S., Hess, P. G., Lamarque, J. F., Pfister, G. G., Fillmore, D., Granier, C., Guenther, A., Kinnison, D., Laepple, T., Orlando, J., Tie, X., Tyndall, G., Wiedinmyer, C., Baughcum, S. L., and Kloster, S.: Description and evaluation of the Model for Ozone and Related chemical Tracers, version 4 (MOZART-4), Geosci. Model Dev., 3, 43-67, 2010.
- Johnson, K. S., Zuberi, B., Molina, L. T., Molina, M. J., Iedema, M. J., Cowin, J. P., Gaspar, D. J., Wang, C., and Laskin, A.: Processing of soot in an urban environment: case study from the Mexico City Metropolitan Area, Atmospheric Chemistry and Physics, 5, 3033-3043, 2005.
- Lamarque, J. F., Bond, T. C., Eyring, V., Granier, C., Heil, A., Klimont, Z., Lee, D., Liousse, C., Mieville, A., Owen, B., Schultz, M. G., Shindell, D., Smith, S. J., Stehfest, E., Van Aardenne, J., Cooper, O. R., Kainuma, M., Mahowald, N., McConnell, J. R., Naik, V., Riahi, K., and van Vuuren, D. P.: Historical (1850-2000) gridded anthropogenic and biomass burning emissions of reactive gases and aerosols:

methodology and application, *Atmospheric Chemistry and Physics*, 10, 7017-7039, DOI 10.5194/acp-10-7017-2010, 2010.

Ma, P. L., Rasch, P. J., Fast, J. D., Easter, R. C., Gustafson, W. I., Liu, X., Ghan, S. J., and Singh, B.: Assessing the CAM5 physics suite in the WRF-Chem model: implementation, resolution sensitivity, and a first evaluation for a regional case study, *Geosci. Model Dev.*, 7, 755-778, 10.5194/gmd-7-755-2014, 2014.

Ma, P. L., Rasch, P. J., Wang, H. L., Zhang, K., Easter, R. C., Tilmes, S., Fast, J. D., Liu, X. H., Yoon, J. H., and Lamarque, J. F.: The role of circulation features on black carbon transport into the Arctic in the Community Atmosphere Model version 5 (CAM5), *Journal of Geophysical Research-Atmospheres*, 118, 4657-4669, 10.1002/jgrd.50411, 2013.

Moteki, N., Kondo, Y., Miyazaki, Y., Takegawa, N., Komazaki, Y., Kurata, G., Shirai, T., Blake, D. R., Miyakawa, T., and Koike, M.: Evolution of mixing state of black carbon particles: Aircraft measurements over the western Pacific in March 2004, *Geophysical Research Letters*, 34, Artn L11803  
Doi 10.1029/2006gl028943, 2007.



## **Response to Anonymous Referee #4**

(Note: Reviewer comments are listed in grey, and responses to reviewer comments are in black. Pasted text from the new version of the paper is in italics.)

This work conducts numerous sensitivity simulations using a global chemical transport model (MOZART-4) by changing the aging timescale of the tagged BC from various geographical source regions. The authors optimize the aging timescale of BC emitted from each source region by minimizing errors in vertical profiles of BC mass mixing ratios between the simulations and HIPPO aircraft measurements. They investigate the contributions of BC from each source region to BC loading over each receptor region, and examine relationship between lifetime of BC and its aging timescale. This study is interesting and scientifically important. The subject is of great interest to ACP. For the most part, the manuscript is written clearly. However, the description and validity of the optimization approach in section 2.5 are not sufficient, which are cause for concern (see Major comments). Once these points are addressed satisfactory, the paper should in my opinion be suitable for publication in ACP.

Major comments:

We greatly appreciate the reviewer for detailed, valuable and constructive comments, especially those regarding the uncertainties of our study. The suggestions are extremely helpful to improving our manuscript.

My main concern is the validity of the optimization approach shown in section 2.5. In definition of the NMAE in equation (3), the authors normalize the absolute errors by the minimum of observed and modeled BC so that NMAE weights both high bias and low bias equally. However, I am not convinced that this approach can estimate the optimized aging timescale of BC. For example, we consider one data point for simplicity in the following two cases: Case A:  $BC_o=4$ ,  $BC_m=2.5$ ;  $NMAE = 1.5/2.5 = 0.6$  (greater NMAE). Case B:  $BC_o=4$ ,  $BC_m = 6$ ;  $NMAE = 2/4 = 0.5$  (smaller NMAE). According to this approach, case B shows better model results because of the smaller NMAE, although I think that case A shows better agreement between the modeled and observed BC values.

I guess that modeled BC ( $BC_m$ ) in equation (3) is sum of the 13 tagged BC from each source region, and contributions of the tagged BC from each region to the total BC over the HIPPO regions are largely different. I think that variations of the BC mass mixing ratio due to changes in the aging timescale are greater for the tagged BC from the large-contributed source regions (e.g., East Asia) and smaller from the small contributed regions. In this case, the approach may have limitations to estimate the optimized aging timescale for BC from the small-contributed regions, because the total BC mixing ratio is dominated by BC from the large-contributed regions. According to Table 1, the optimized aging timescales are 4 hours for BC from the large-contributed source regions (page 16959, lines 4-5) and are greater values (120-200 hours) from the small-contributed regions.

If I am misunderstanding the optimization approach, the authors should clarify their approach and

discuss the validity of their approach.

The reviewer’s understanding towards the optimization approach is correct. To clarify the procedure, we expanded the description of the optimization approach in Section 2.5:

*“We perform 13 simulations, each with different constant aging timescales (i.e. 4, 8, 12, 18, 24, 27.6, 38.4, 48, 60, 90, 120, 160 or 200 hours). Every simulation tags BC from each of 13 regions (i.e., North America, East Asia, Canada, ...); as mentioned in Section 2.3,  $BC_m(j,k)=\sum_r BC_m(j,k,r)$ , where  $r$  denotes each region. We construct  $BC_m(j,k)$  using all possible combinations of  $BC_m(j,k,r)$  from the 13 simulations. Then we check which combination of  $BC_m(j,k,r)$  best matches BC observations. Note that we constrain the aging rates of BC emitted from Africa, South America, and Australia to be the same since these three regions are all biomass burning dominated sources in the Southern Hemisphere, which effectively reduces the total number of tagged tracers from 13 to 11. Thus, we determine the best-fit BC aging timescale for each source region (out of  $13^{11}$  combinations in total) that minimizes MNAE.”*

We agree with the reviewer that there are multiple limitations in our original optimization scheme. As the reviewer mentioned, our modeled BC concentration is the sum of 13 regions which is typically dominated by only one or a few source regions for each place. Therefore, our optimization on BC aging is more accurate to these tracers emitted nearby than those experienced longer-distance transport. To differentiate the uncertainties of the optimized aging timescales for different regions, we add an additional table in the supplementary materials to represent the range of each optimized aging timescale (see Table S1 in the Supplementary material or below). For example, during HIPPO1, the optimized aging timescale for Middle Asian BC is 120 hours, but the uncertainty range is 4-200 hours, much broader than the aging timescale of EA tracer (4-4).

Table S1. Range of plausible aging timescales (units = hours) for 13 regions (For each HIPPO campaign, we assign a range of BC aging timescales for a region if the corresponding MNAE value is no larger than that of the optimized MNAE plus a small perturbation  $\Delta E=0.01$ ).

		CA	SU	EU	MA	EA	ME	NA	SE	IN	AF	SA	AU	RR
<b>HIPPO1</b>	Jan	12-200	4-200	90-120	4-200	4-8	4-60	160-200	4-4	4-8	4-4	4-160	4-60	90-120
<b>HIPPO2</b>	Nov	90-200	4-200	120-160	4-200	4-4	4-60	4-24	4-8	4-8	4-90	90-200	90-160	160-200
<b>HIPPO3</b>	Apr	4-200	60-200	200-200	4-200	38. 4-48	160-200	4-60	27. 6-48	4-48	18-90	18-60	4-27. 6	200-200
<b>HIPPO4</b>	Jun	38. 4-90	4-18	120-200	4-200	4-8	4-200	4-18	4-8	4-48	4-38. 4	4-120	4-8	200-200
<b>HIPPO5</b>	Aug	90-120	4-4	4-38. 4	4-120	4-4	4-60	4-4	4-4	4-12	60-90	60-60	48-160	4-4

We agree with the reviewer that our optimized aging timescales are more robust for specific regional BC tracers than others, therefore we added following discussions on the uncertainties in optimized aging timescales in Section 6:

*“...Fourthly, the computed optimized aging rate is more accurate for tracers (i.e. source regions) with larger emissions and in closer proximity to the Pacific Ocean (e.g. East Asia). This is because modeled BC concentrations over the Pacific (i.e. the location of HIPPO observations) for each latitude and longitude bin are typically dominated by only a few source regions, and the*

*sensitivity of MNAE on each regional BC tracer is different (see Figure S5 in the supplementary material). For some source regions, observations in other remote regions would provide a better constraint for optimizing aging timescale in the model. More specifically, aircraft observations over the Atlantic Ocean could better constrain aging timescales for BC emitted from Africa and South America. As new observations become available, this study could be repeated to more accurately optimize the aging timescale for source regions with lower relative contributions to BC over the Pacific (e.g. Middle Asia)...”*

If possible, in addition to the present approach, it would be better to optimize the BC aging rate by other conventional approaches (e.g., mean normalized gross error, normalized mean error for each altitude range, Taylor diagram, etc.) and evaluate the statistical values in a comprehensive manner, which could give the confidence in the validity of the estimates. If these evaluations are difficult, the authors should at least address limitations of their approach and discuss possible errors included in their results.

Excellent suggestion! In the previous example given by the reviewer:

“Case A:  $BC_o=4$ ,  $BC_m=2.5$ ;  $NMAE = 1.5/2.5 = 0.6$  (greater NMAE). Case B:  $BC_o=4$ ,  $BC_m = 6$ ;  $NMAE = 2/4 = 0.5$  (smaller NMAE). According to this approach, case B shows better model results because of the smaller NMAE, although I think that case A shows better agreement between the modeled and observed BC values.”

We find that for this example, statistical values like mean absolute error normalized by observed value ( $MNAE_o$ ) and mean absolute error normalized by the average of observed and modeled values ( $MNAE_a$ ) will show a better agreement for case A than case B, the same as the reviewer expected. Following the reviewer’s suggestion, we conduct additional tests with  $MNAE_o$  and  $MNAE_a$ , re-generated optimized BC aging timescales, and added the following tables to the supplementary material:

Table S2. Optimized aging timescales (units = hours) for 13 regions using  $MNAE_o =$

$$\frac{1}{N} \sum_{nlat} \sum_{nalt} \frac{Abs(BC_m(j,k) - BC_o(j,k))}{BC_o(j,k)}$$

	CA	SU	EU	MAEA	ME	NA	SE	IN	AF	SA	AU	RR
<b>HIPPO1</b> Jan	60	60	120	60	4	12	4	4	4	4	4	4
<b>HIPPO2</b> Nov	200	90	60	4	4	4	4	4	4	4	4	8
<b>HIPPO3</b> Apr	120	200	200	200	38	4	4	18	4	12	12	27
<b>HIPPO4</b> Jun	18	4	200	4	4	200	4	4	4	4	4	4
<b>HIPPO5</b> Aug	8	4	4	4	4	4	4	4	4	4	4	4

Table S3. Optimized aging timescales (units = hours) for 13 regions using  $MNAE_a =$

$$\frac{1}{N} \sum_{nlat} \sum_{nalt} \frac{Abs(BC_m(j,k) - BC_o(j,k))}{(BC_m(j,k) + BC_o(j,k))/2}$$

		CA	SU	EU	MA	EA	ME	NA	SE	IN	AF	SA	AU	RR
<b>HIPPO1</b>	Jan	200	200	90	200	4	200	120	4	4	18	18	18	4
<b>HIPPO2</b>	Nov	200	200	48	200	4	4	4	4	4	90	90	90	160
<b>HIPPO3</b>	Apr	200	200	200	200	38	200	4	24	60	12	12	12	200
<b>HIPPO4</b>	Jun	18	8	200	200	4	160	4	4	4	4	4	4	160
<b>HIPPO5</b>	Aug	120	4	38	4	4	4	4	4	4	90	90	90	4

Comparing Table S2, S3 to Table 1, the optimized results are similar to those using the originally defined  $MNAE_m$  which is normalized by the minimum of BCo and BCm, as shown below. Generally, they all show a longer aging timescale in high-latitude regions and a shorter aging timescale for other regions, although moderate differences do exist.

		CA	SU	EU	MA	EA	ME	NA	SE	IN	AF	SA	AU	RR
<b>HIPPO1</b>	Jan	200	90	120	120	4	12	160	4	4	4	4	4	90
<b>HIPPO2</b>	Nov	200	160	160	90	4	4	4	4	4	90	90	90	200
<b>HIPPO3</b>	Apr	200	200	200	200	38	200	4	38	27	24	24	24	200
<b>HIPPO4</b>	Jun	60	4	160	12	4	160	4	4	4	4	4	4	200
<b>HIPPO5</b>	Aug	120	4	18	4	4	4	4	4	4	60	60	60	4

In general, we hope we can find a statistic which can judge model performance in both polluted and clean conditions since the latter usually cover a much broader spatial extent. Orders of magnitude overestimation or underestimation in these clean regions (though the absolute values are small) may also indicate large model biases which need further investigation. Thus, we normalize the absolute errors by the minimum of observed and modeled BC so that  $MNAE_m$  weights both high bias and low bias equally. However, we agree with the reviewer that which error matrix we choose influences the optimization results and acknowledged this issue in Section 6:

*“...Thirdly, the optimized aging results may somewhat depend on the error matrix chosen. We conduct additional simulations with different error matrices (see Table S2, S3 in supplementary material). The results are overall similar, but in some cases moderate differences are found...”*

The authors chose the aging timescale between 4 hours and 200 hours in section 2.5. On the other hand, Table 1 shows that the best-fit aging timescales are 4 hours and 200 hours in many cases (minimum or maximum). I believe that conclusions of this paper (e.g., faster aging over the anthropogenic source regions and slower aging over high latitude regions) will not be changed even if the authors expand the range of the timescale, however the authors need to discuss the validity of their estimation.

We also agree with the reviewer that our approach do have limitations and the optimized results may partially depend on the performance of modeling processes beyond aging. In addition, this study only used 13 choices of aging timescales for regions, which cannot cover all the possibilities happening in the real atmosphere. Thus, every given number may actually represent a range. For example, ‘4h’ and ‘200h’ in Table 1 can mean ‘less than 8h’(or fast aging) and ‘greater than 160 hours’ (or slow aging), respectively. Nevertheless, the goal of our aging optimization is not to provide a set of accurate aging timescales that can be directly used in models, but to utilize every HIPPO observation at most to inform the possible spatiotemporal pattern of aging timescales globally. Our results may indicate that the aging rate of BC may change by region and season, as opposed to a fixed aging timescale currently widely used in many chemical transport models. In addition, we extensively expanded the caveats on Section 6 to address the uncertainties of our approach:

We followed the reviewer’s suggestions and added more discussion in Section 6:

*“We note that there are multiple limitations to our approach. Firstly, we assume that model parameterizations of wet and dry deposition, precipitation, transport, and emissions are realistic, even though these processes also affect BC distributions and have uncertainties (Vignati et al., 2010; Fan et al., 2012). Consequently, the optimized aging timescales may partially counter biases in these processes (i.e. other than aging), and may vary according to the model used. For example, as model resolution increases, aerosol-cloud interactions in climate models can be better resolved, which can improve the simulation of BC transport (Ma et al., 2013; Ma et al., 2014). Therefore, the optimized aging timescales might change if models with different cloud schemes or spatial resolutions are used. Secondly, due to limitations in computing resources, we carry out simulations assuming 13 discrete values for aging timescale. Optimized aging timescale could have been more precisely determined with more simulations... The goal of the optimization presented here is not to provide precise aging timescales that can be directly used in models, since models differ significantly in their parameterizations of physical and chemical processes, particularly the wet scavenging. Also, BC aging includes complicated chemistry and physics, but is simplified in our modeling as a first-order conversion from hydrophobic to hydrophilic BC. Nevertheless, this study proposes a useful method to utilize all HIPPO observations and explore the spatiotemporal pattern of BC aging timescales globally.”*

The authors should improve the description of the optimization approach in section 2.5. Please clarify how the 13 tagged BC are used in equation (3).

We expanded the description of optimization approach in section 2.5:

*“We perform 13 simulations, each with different constant aging timescales (i.e. 4, 8, 12, 18, 24, 27.6, 38.4, 48, 60, 90, 120, 160 or 200 hours). Every simulation tags BC from each of 13 regions (i.e., North America, East Asia, Canada, ...); as mentioned in Section 2.3,  $BC_m(j,k) = \sum_r BC_m(j,k,r)$ , where  $r$  denotes each region. We construct  $BC_m(j,k)$  using all possible*

*combinations of  $BC_m(j, k, r)$  from the 13 simulations. Then we check which combination of  $BC_m(j, k, r)$  best matches BC observations. Note that we constrain the aging rates of BC emitted from Africa, South America, and Australia to be the same since these three regions are all biomass burning dominated sources in the Southern Hemisphere, which effectively reduces the total number of tagged tracers from 13 to 11. Thus, we determine the best-fit BC aging timescale for each source region (out of  $13^{11}$  combinations in total) that minimizes MNAE.”*

Please describe the time information for the modeled and observed BC. Are these compared the same time? Please indicate time resolution of the observation data and model output (hourly, daily, monthly?) used in equation (3).

We compared the daily model output to the HIPPO observational data. We have clarified this issue in the revised manuscript. Please see section 2.5 or the revised text below:

*“The model output daily averaged BC mixing ratios. For every record in HIPPO data (averaged in every 10s), we find modeled BC mixing ratio at the same longitude, latitude, altitude, and on the same day correspondingly. In this way, modeled and observed BC mixing ratios are paired, and then are averaged respectively over latitude and altitude bins. ”*

Additional comments:

Page 16951, line 14, "with 28 vertical levels": Please indicate the top boundary of the model..

We added the corresponding information in the revised manuscript (i.e., Section 2.1):

*“ ...The model is run at a horizontal resolution of approximately  $1.9^\circ \times 1.9^\circ$  (latitude  $\times$  longitude) with 28 vertical levels from surface to approximately 2 hPa... ”*

Page 16951, lines 15-16: Is MACCity inventory (Lamarque et al., 2010) used for the CMIP5 project?

According to the website [http://accent.aero.jussieu.fr/MACC\\_metadata.php](http://accent.aero.jussieu.fr/MACC_metadata.php), “As part of two projects funded by the European Commission, MACC and CityZen, the ACCMIP and the RCPs emissions dataset have been adapted and extended on a yearly basis for the period 1990-2010. For anthropogenic emissions, emission data were interpolated on a yearly basis between the base years 1990, 2000, 2005 and 2010. For the years 2005 and 2010, the RCP 8.5 emissions scenario was chosen (4 emissions scenarios were developed in support of the IPCC-AR5: RCP 2.6, RCP 4.5, RCP 6, RCP 8.5). This 'extension' of the ACCMIP and RCPs emission dataset for the MACC and CityZEN projects is referred to as MACCity (MACC/CityZen) emission dataset.” We modified the sentence (in Section 2.1) to make it more precise:

*“...Anthropogenic emissions are based on the MACCity emission inventory (<http://www.pole-ether.fr/eccad>), which is extended from the database used for IPCC Coupled Model*

*Intercomparison Project (Lamarque et al., 2010). ”*

Page 16951, lines 9-10: Does "C" include ice content?

Yes, C is the sum of ice and liquid water content. We revised this sentence in Section 2.2 to make it clearer:

*“...C is the sum of cloud ice and liquid water content ( $\text{kg}\cdot\text{m}^{-3}$ )...”*

Page 16954, lines 12-13: Please show a few references at the end of the sentence.

Thanks, we added some references at this place, namely:

*Y., Shiraiwa, M., Gong, Y. G., Shao, M., Hu, M., Zhu, T., Zhang, Y. H., Carmichael, G. R., Wiedensohler, A., Andreae, M. O., and Poschl, U.: Size-resolved measurement of the mixing state of soot in the megacity Beijing, China: diurnal cycle, aging and parameterization, Atmospheric Chemistry and Physics, 12, 4477-4491, DOI 10.5194/acp-12-4477-2012, 2012.*  
*Moteki, N., Kondo, Y., Miyazaki, Y., Takegawa, N., Komazaki, Y., Kurata, G., Shirai, T., Blake, D. R., Miyakawa, T., and Koike, M.: Evolution of mixing state of black carbon particles: Aircraft measurements over the western Pacific in March 2004, Geophysical Research Letters, 34, Artn L11803*

Page 16954, line 28: Schwarz et al. (2008"b") is not shown in the reference list.

Thanks for catching this mistake. We changed the citation here to (*Schwarz et al., 2008*), which is now in the reference list.

Page 16958, lines 6, Figure S1: Typo? Figure S3 in the present manuscript?

Thanks for catching this typo. It should be Figure S3 in the previous manuscript. We have fixed it.

Page 16958, lines 14-21: In the Southern Hemisphere during HIPPO5 (Figure 4), the improved BC (green) is smaller than the observed BC (black), however the original BC (red) is greater than the observed BC. If the model does not capture abrupt biomass burning emission events, the original BC would also be smaller than the observed BC. I am not satisfied with the author's explanation, because differences in modeled BC values (green and red) are caused mainly by the wet deposition of BC.

Excellent point! We agree with the reviewer that factors such as wet removal also significantly influence the BC distribution. Since this study assumes BC aging timescales in all the southern hemispheric countries are the same, it may not be able to differentiate variability of BC aging across regions in the southern hemisphere. In addition, the optimized aging in these regions exhibit large uncertainties and may require additional aircraft campaigns over the Atlantic Ocean as well as the Indian Ocean to better calibrate the BC timescales in the southern hemisphere. In the revised manuscript, we followed the reviewer's suggestion and revised the whole paragraph.



Now we have the following discussions in Section 3:

*“In a few cases, relatively large differences between the improved model and observations remain. These differences could be attributed to any number of factors (e.g., emissions, transport, cloud/precipitation, aging process, wet removal efficiency, etc.). For example, models could misrepresent BC wet deposition, originating from biases in precipitation. As shown in Figures S4 in the supplementary materials, though MOZART-4 generally captures well the spatial extent of precipitation during all HIPPO campaigns, biases occasionally appear when comparing to the NCEP reanalysis over the western Pacific. As another example, the model uses a monthly biomass burning emission inventory. This means that modeled emissions lack daily variation in biomass burning activities that could be important where biomass burning emissions dominate BC loading. Underestimates in BC mixing ratio may be partially due to abrupt emissions events that are not captured by the model. Lastly, since this study assumes that BC aging timescale in all the southern hemispheric continents is the same, we do not account for variability in BC aging rates from these regions that may exist in reality. ”*

Equation (3) and Table 1, terminology: "Normalized mean absolute error (NMAE)" should be "mean normalized absolute error"? "Normalized mean bias (NMB)" should be "mean normalized bias" or "mean fractional bias"?

Thanks for correcting this. We have corrected all the uses of these terms in the paper. Now we are using mean normalized absolute error (MNAE) and mean normalized bias (MNB).

# Long-range transport of black carbon to the Pacific Ocean and its dependence on aging timescale

J. Zhang<sup>1,2,3</sup>, J. Liu<sup>1</sup>, S. Tao<sup>1</sup>, and G. A. Ban-Weiss<sup>3</sup>

[1] Laboratory for Earth Surface Processes, College of Urban and Environmental Sciences, Peking University, Beijing, China

[2] School of Physics, Peking University, Beijing, China

[3] Department of Civil and Environmental Engineering, University of Southern California, Los Angeles, CA, USA

Correspondence to: J. Liu (E-mail: [jfliu@pku.edu.cn](mailto:jfliu@pku.edu.cn))

## Abstract

Improving the ability of global models to predict concentrations of black carbon (BC) over the Pacific Ocean is essential to evaluate the impact of BC on marine climate. In this study, we tag BC tracers from 13 source regions around the globe in a global chemical transport model MOZART-4. Numerous sensitivity simulations are carried out varying the aging timescale of BC emitted from each source region. The aging timescale for each source region is optimized by minimizing errors in vertical profiles of BC mass mixing ratios between simulations and HIAPER Pole-to-Pole Observations (HIPPO). For most HIPPO deployments, in the Northern Hemisphere, optimized aging timescales are less than half a day for BC emitted from tropical and mid-latitude source regions, and about 1 week for BC emitted from high latitude regions in all seasons except summer. We find that East Asian emissions contribute most to the BC loading over the North Pacific, while South American, African and Australian emissions dominate BC loadings over the South Pacific. Dominant source regions contributing to BC loadings in other parts of the globe are also assessed. The lifetime of BC originating from East Asia (i.e., the

world's largest BC emitter) is found to be only 2.2 days, much shorter than the global average lifetime of 4.9 days, making East Asia's contribution to global burden only 36% of BC from the second largest emitter, Africa. Thus, evaluating only relative emission rates without accounting for differences in aging timescales and deposition rates is not predictive of the contribution of a given source region to climate impacts. Our simulations indicate that lifetime of BC increases nearly linearly with aging timescale for all source regions. When aging rate is fast, the lifetime of BC is largely determined by factors that control local deposition rates (e.g. precipitation). The sensitivity of lifetime to aging timescale depends strongly on the initial hygroscopicity of freshly emitted BC. Our findings suggest that the aging timescale of BC varies significantly by region and season, and can strongly influence the contribution of source regions to BC burdens around the globe. Therefore, improving parameterizations of the aging process for BC is important for enhancing the predictive skill of global models. ~~Improving parameterizations of the aging process for BC is important for enhancing the predictive skill of air quality and climate models.~~ Future observations that investigate the evolution of hygroscopicity of BC as it ages from different source regions to the remote atmosphere are urgently needed.

## 1 Introduction

Black carbon (BC) is an efficient absorber of solar radiation and therefore heats the atmosphere and the Earth surface (Ramanathan and Carmichael, 2008). Estimates of BC's direct radiative forcing widely vary, ranging from  $0.19 \text{ W/m}^2$  by Wang et al (2014) to  $0.88 \text{ W/m}^2$  by Bond et al. (2013). The Intergovernmental Panel on Climate Change Fifth Assessment Report (IPCC AR5) assesses the direct radiative forcing of BC to be  $0.40 \text{ W/m}^2$  with a large uncertainty range of 0.05 to  $0.80 \text{ W/m}^2$ . Besides its direct radiative effects, BC also affects Earth's energy budget indirectly by influencing cloud formation (Koch and Del Genio, 2010) and snow albedo (Hansen and Nazarenko, 2004;Flanner et al., 2007;He et al., 2014), although these processes are relatively less understood and subject to greater uncertainties. In addition, epidemiological studies have shown

that BC is associated with increased hospital admissions and premature mortalities (Bell et al., 2009;Janssen et al., 2011).

Relative to greenhouse gases, BC has a shorter lifetime, and its concentration changes considerably by location and season (Liu et al., 2011). Horizontal and vertical distributions of BC are not well constrained with observations, contributing to the uncertainties in estimates of BC's radiative forcing (Bond et al., 2013). BC has higher radiative forcing efficiency (i.e. radiative forcing per unit mass of BC) when its underlying surface is highly reflective (e.g. cloud, snow and ice). The radiative forcing of BC also depends on its attitude, and is enhanced if located above clouds relative to below clouds (Satheesh, 2002;Zarzycki and Bond, 2010). The direct radiative forcing efficiency of BC may increase by a factor of 10 as altitude increases from the surface to the lower stratosphere (Samset and Myhre, 2011), whereas forcing associated with the semi-direct effect (i.e. changes in cloudiness due to local heating from BC) becomes more negative as altitude increases (Samset and Myhre, 2015). On the other hand, the climate response of BC depends on altitude in different ways than forcing. Since BC warms its surroundings, near-surface BC can warm the surface more than BC at high altitudes, even though the high-altitude BC has higher top-of-atmosphere direct radiative forcing efficiency. BC at high altitudes could even cause surface cooling (Ban-Weiss et al., 2012;Samset et al., 2013). Near-surface BC has also been found to increase precipitation, whereas BC at higher altitudes can suppress precipitation (Ming et al., 2010;Ban-Weiss et al., 2012;Samset and Myhre, 2015).

BC over oceans could potentially play a significant role in changing the marine climate through influences on the top-of-atmosphere and surface energy balance, as well as temperature and cloud profiles. For instance, BC over the Arabian Sea has been shown to dim the surface, decrease sea surface temperature, reduce monsoon circulation and vertical wind shear, and consequently increase the intensity of cyclones (Evan et al., 2011). The Pacific Ocean is the largest ocean in the world, extending from the Arctic to the Antarctic. Its marine climate has been shown to influence the weather and environment in neighboring continents, for example the South Asian and East Asian summer monsoon (Bollasina et al., 2011;Lau and Nath, 2012;Liu et al.,

2013b;Bollasina et al., 2014). Recently, the HIAPER Pole-to-Pole Observation (HIPPO) campaign has enabled further research on trans-Pacific transport of BC. HIPPO's five deployments provide new constraints for modelling the vertical structures of BC at a wide range of latitudes over the Pacific spanning all seasons (Wofsy et al., 2011;Kipling et al., 2013). Past model inter-comparison studies have shown that a collection of global models predict BC concentrations that are a factor of 3 and 10 higher than HIPPO observations in the lower and upper troposphere, respectively (Schwarz et al., 2013); the vertical profiles simulated by the 15 global models markedly differ (Samset et al., 2014).

The aforementioned inter-model differences and disagreement between models and HIPPO observations can be attributed to the uncertainties in emissions and meteorology, along with different treatments of convective transport and deposition (Koch et al., 2009;Vignati et al., 2010). Wet scavenging processes are a major source of uncertainty in predicting BC concentrations over remote regions (Textor et al., 2007;Schwarz et al., 2010). As emitted, BC is mostly hydrophobic (Laborde et al., 2013), but can become coated by water-soluble components through atmospheric aging processes. The coatings transits BC from being hydrophobic to hydrophilic, allowing the BC-containing particles to become cloud condensation nuclei and be scavenged by precipitation (Riemer et al., 2010;Oshima and Koike, 2013). Exponential timescale for this aging process to occur, the so-called "aging timescale", which is also the reciprocal of aging rate, therefore highly influences the timing of cloud formation and wet deposition, and thus is of great research interest (Liu et al., 2011). The thickness of BC coatings have been observed to increase with aging at the remote marine Pico Mountain Observatory, which shows that the fraction of coated particles for plumes with an age of ~15.7 days is 87%, higher than that of ~9.5 days (57%) (China et al., 2015). Quantitatively relating the age of BC-containing particles to its hygroscopicity using observations is very challenging (McMeeking et al., 2011). Laboratory measurements show that BC particles are considerably hygroscopic after being coated by condensed H<sub>2</sub>SO<sub>4</sub> (Zhang et al., 2008), or when a sulfur-containing compound is added to the diesel fuel itself, presumably also leading to a sulfuric coating (Lammel and Novakov, 1995). The oxidation of organic coatings on

BC by ozone and nitrogen oxide is also highlighted as an important pathway to aging in chamber studies (Kotzick et al., 1997;Kotzick and Niessner, 1999). Another study reporting observations in the United Kingdom finds that nitrate is the primary component of the coating on BC that leads to substantial increases in hygroscopicity (Liu et al., 2013a). In principle, the conversion of hydrophobic to hydrophilic BC is very complicated, involving coagulation with sulfate and nitrate, condensation of nitric and sulfuric acid, and oxidation of organic coatings (Riemer et al., 2004;Matsui and Koike, 2012).

The aforementioned uncertainties in process and timescale for atmospheric aging, which converts BC from being hydrophobic to hydrophilic, leads to significant uncertainties in the transport of BC from source regions to remote areas. For example, previous studies that look at source regions of Arctic BC disagree on the relative importance of contributions from North American, Asian, and European emissions (Koch and Hansen, 2005;Shindell et al., 2008;Bourgeois and Bey, 2011;Wang et al., 2014). BC over the North Pacific Ocean is significantly influenced by the long-range transport of BC from Asia (Kaneyasu and Murayama, 2000). Eastern and Central Asia is regarded as the most significant contributor to BC burden above the oceans in the Northern Hemisphere (Ma et al., 2013a). However, the source of BC over the Pacific Ocean at different latitudes and altitudes remains unclear.

The major objectives of this study are to understand the sensitivity of BC aging timescale on its loading and source attribution using a global chemical transport model. We quantify the relative contributions of 13 source regions to BC loadings around the globe, with a focus on BC over the Pacific Ocean. In section 2, we improve the model by implementing physically-based dry and wet deposition schemes. We also tag BC emitted from different source regions and conduct sensitivity tests to investigate how different aging timescales affect spatial (i.e. horizontal and vertical) distributions and source-receptor relationships for BC. In section 3, we optimize the aging timescale of BC for each source region to attain the best match to HIPPO observations. Section 4 identifies the most significant contributors to BC over the Pacific Ocean, and quantifies

the source-receptor relationship. We also discuss the relationship between lifetime and aging timescales of BC in section 5.

## 2 Method

### 2.1 Model description and configuration

In this research, we use the Model for Ozone and Related Chemical Tracers, version 4 (MOZART-4) (Emmons et al., 2010), a global chemical transport model developed at the National Center for Atmospheric Research (NCAR) (Emmons et al., 2010). Built on the framework of the Model of Atmospheric Chemistry and Transport (Rasch et al., 1997) (MATCH) (Rasch et al., 1997) with a series of updates, MOZART-4 resolves horizontal and vertical transport, chemistry, and dry and wet deposition of 85 gas-phase and 12 bulk aerosol species. Vertical transport considers both diffusion in the boundary layer using the Holtslag and Boville (1993) scheme, and convective mass flux using the Hack (1994) scheme for shallow and middle convection, and the Zhang and McFarlane (1995) scheme for deep convection. Horizontal transport is characterized by a semi-Lagrangian advection scheme (Lin and Rood, 1996) with a pressure fixer (Horowitz et al., 2003). In the standard model, BC is represented by two classes of tracers: hydrophobic and hydrophilic. Hydrophobic BC accounts for 80% of BC emissions and converts to hydrophilic BC with an exponential aging timescale of about 1.6 days. Only hydrophilic BC can be wet scavenged. Its first order wet scavenging rate is set to 20% of that for nitric acid, and is proportional to precipitation rate. Precipitation is produced by stratiform clouds (i.e. large-scale precipitation) and convective clouds (i.e. convective precipitation). Dry deposition velocity for both BC tracers is set to  $0.1 \text{ cm s}^{-1}$  (Emmons et al., 2010).

The model is run at a horizontal resolution of approximately  $1.9^\circ \times 1.9^\circ$  (latitude  $\times$  longitude) with 28 vertical levels from surface to approximately 2 hPa, and is driven by NCEP reanalysis meteorology. Anthropogenic emissions are based on the MACCity emission inventory



(<http://www.pole-ether.fr/eccad>), [which is extended from the database used for IPCC Coupled Model Intercomparison Project \(Lamarque et al., 2010\)](#), ~~which is developed for IPCC AR5 experiments (Granier et al., 2011)~~. Biomass burning emissions are acquired from the Global Fire Emissions Database (GFED) version 3 (van der Werf et al., 2010). Model simulations are for January 1, 2008 to December 31, 2011, and the first year of the simulation is discarded as model spin-up.

## 2.2 Dry and wet deposition schemes

To improve model performance, we employ the dry deposition parameterization (equation 1) from Gallagher et al. (2002)

$$v_d = \frac{1}{r_a + r_s}, \quad r_s = (u^*(0.001222 \log(z_0) + 0.0009 \left(\frac{z_i}{L}\right)^{\frac{2}{3}} + 0.003906))^{-1} \quad (1)$$

where  $v_d$  is dry deposition rate ( $\text{m s}^{-1}$ ),  $r_a$  is aerodynamic resistance,  $r_s$  is surface resistance,  $u^*$  is friction velocity ( $\text{m s}^{-1}$ ),  $z_0$  is the roughness length (m),  $z_i$  is boundary layer depth (m), and  $L$  is the Monin-Obukhov length (m). As a result, dry deposition velocity depends on surface properties (e.g. vegetation type).

For in-cloud wet scavenging of BC, we follow the parameterization used in Liu et al. (2011). The first-order in-cloud scavenging rate coefficient ( $\text{s}^{-1}$ ) is expressed as

$$K_{\text{in}} = \frac{P_{\text{rain}}F_{\text{liq}} + P_{\text{snow}}F_{\text{ice}} + P_{\text{conv}}F_{\text{conv}}}{C} \quad (2)$$

where  $P_{\text{rain}}$ ,  $P_{\text{snow}}$ , and  $P_{\text{conv}}$  are the rates of stratiform rain precipitation, stratiform snow precipitation, and convective precipitation ( $\text{kg m}^{-3} \text{s}^{-1}$ ), respectively, and  $C$  is ~~the cloud water content~~ [the sum of cloud ice and liquid water content](#) ( $\text{kg m}^{-3}$ ). For convective clouds,  $F_{\text{conv}}$  is the fraction of in-cloud hydrophilic BC that is incorporated into cloud droplets or ice crystals. For stratiform clouds,  $F_{\text{liq}}$  ( $F_{\text{ice}}$ ) is the fraction of in-cloud hydrophilic BC that is incorporated into liquid cloud droplets (ice crystals).

As previous studies indicate, the fraction of BC that is incorporated in cloud droplets or ice crystals decreases as temperature decreases and ice mass fraction increases in mixed-phase clouds (Croft et al., 2010; Liu et al., 2011; Croft et al., 2012; Fan et al., 2012). This phenomenon is

attributable to the so-called Bergeron process, by which ice crystals grow rapidly at the expense of liquid droplets, leaving BC-containing cloud nuclei interstitial (i.e. not activated) (Cozic et al., 2007). However, the Bergeron process is not important in deep convective clouds where ice forms rapidly via rimming or accretion. Thus, generally  $F_{\text{ice}} < F_{\text{liq}} < F_{\text{conv}}$ . In this study, we set  $F_{\text{ice}}=0.1$ ,  $F_{\text{liq}}=0.5$ , and  $F_{\text{conv}}=1.0$  as referenced to previous studies (Liu et al., 2011; Wang et al., 2011; Hodnebrog et al., 2014).

### **2.3 HIAPER Pole-to-Pole Observations**

The HIPPO campaigns unprecedentedly provide vertical profiles from the surface to upper troposphere for 26 species over the Pacific Ocean, spanning from approximately 90 °N to 70 °S, in different seasons (Wofsy et al., 2011). BC is measured by a Single Particle Soot Photometer (SP2) using laser-induced incandescence (Schwarz et al., 2010). The SP2 heats BC-containing particles to its vaporization temperature and measures the resulting incandescence emitted by the BC core. Since the intensity of incandescence responds linearly to the mass of refractory BC, SP2 measures BC mass independent of particles morphology and mixing state (Schwarz et al., 2006; Schwarz et al., 2008). We constrain and evaluate our model by comparing simulated vertical profiles of BC mass mixing ratios over the central Pacific Ocean to observations from five field deployments (HIPPO I on January 8<sup>th</sup> – January 30<sup>th</sup>, 2009; HIPPO II on October 31<sup>th</sup> – November 22<sup>th</sup>, 2009; HIPPO III on March 24<sup>th</sup> - April 16<sup>th</sup>, 2010; HIPPO IV on June 14<sup>th</sup> - July 11<sup>th</sup>, 2011; HIPPO V on August 9<sup>th</sup> – September 9<sup>th</sup>, 2011). Note that we use only the HIPPO observations taken in the Central Pacific Ocean (130 °W - 160 °E) and ignore observations near source regions.

### **2.4 Tracer tagging and sensitivity simulations**

In this study, we add 13 tracers to the model to explicitly track BC emissions from non-overlapping geopolitical regions, an approach often called “tagging” (Rasch et al., 2000). Tagging is more accurate and less computationally consuming than the widely used emission sensitivity approach (Wang et al., 2014). We expand the ten defined continental regions in Liu et

al (2009) to thirteen source regions to better distinguish the differences in climate and emission source type between regions. As shown in Figure 1, the tagged source regions are Canada (CA), North America except Canada (NA), East Asia (EA), the former Soviet Union (SU), Europe (EU), Africa (AF), South America (SA), the Indian subcontinent (IN), Australia (AU), Middle Asia (MA), Southeast Asia (SE), the Middle East (ME), and the rest regions (RR). For each simulation, the tagged tracers undergo transport and deposition processes in the same way as untagged BC.

Since all the chemical and physical processes involving BC are nearly linear in MOZART-4, the relative difference between the sum of the 13 regional BC tracers and the untagged BC is small (i.e., in most cases less than 1% with the largest biases less than 4%). Therefore, the sum of the 13 regional BC tracers is approximately equal to the untagged BC.

In the model, two parameters control the hygroscopicity of BC: initial fraction of hydrophilic BC in freshly emitted BC (20%), and a fixed e-folding aging timescale, which characterizes the timescale for conversion of hydrophobic BC to hydrophilic BC in the atmosphere.

Hygroscopicity of BC-containing particle determines whether BC can be wet scavenged, and thus affects the lifetime of BC. Therefore, constraining the aging timescale is essential for accurately simulating long-range transport and atmospheric concentrations of BC. In global models, e-folding aging timescale is often fixed at 1.2 or 1.6 days (27.6 or 38.4 h), even though studies find it can vary from several hours to 2 weeks in different regions (Liu et al., 2011; Shen et al., 2014). So we conduct 13 sensitivity simulations with different e-folding aging timescales (i.e. 4, 8, 12, 18, 24, 27.6, 38.4, 48, 60, 90, 120, 160, and 200 hours). Note that while we define aging timescale as that for converting BC from hydrophobic to hydrophilic, some other studies use this term to describe the change from thinly to thickly coated BC (Moteki et al., 2007; Saikawa et al., 2009).

## 2.5 Optimization of BC aging rate-timescale to match HIPPO observations

The conversion of hydrophobic BC to hydrophilic BC in global chemistry transport models is often expressed by a fixed exponential aging timescale of 1 to 2 days (e.g. 1.2 days in

GEOS-chem, 1.6 days in MOZART-4) (Feng, 2007;Wang et al., 2011). However, previous studies have indicated that the aging rate of BC varies spatially and temporally due to different atmospheric photochemical conditions and co-emitted species (Liu et al., 2011;Huang et al., 2013;Shen et al., 2014). Aging rate peaks during summer daytime and in low-latitude regions because high OH concentrations promote the production of water-soluble condensable species. The aging rate is slower at night and during winter because OH concentrations are low and thus coagulation, which is slower than condensation, dominates the formation of internally mixed BC (Riemer et al., 2004;Liu et al., 2011;Bian et al., 2013). Observations show that biomass burning emitted BC, compared with urban BC, has larger number fraction of coated particles (70% versus 9%) and thicker coatings (65nm versus 20nm), ~~implying that it is more susceptible to wet deposition~~ (Schwarz et al., 2008b). Different source regions are distinct in their source types (e.g. anthropogenic, biomass burning) and concentrations of oxidants. Therefore, BC emitted from different regions should undergo aging with different timescales.

In this study, we optimize the aging timescales of BC emitted from thirteen source regions to best match the HIPPO observations. For each HIPPO deployment, we compare observations versus simulations from 70 °S to 90 °N and 0 to 10km along the HIPPO trajectory. The absolute deviation between modeled BC ( $BC_m$ ) and observed BC ( $BC_o$ ) mass mixing ratios for each latitude and altitude is calculated, and the average of ~~normalized~~ mean normalized absolute error (NMNAE) is then used as an indicator of the model performance in each deployment:

$$\underline{NMNAE} = \frac{1}{N} \sum_{nlat} \sum_{nalt} \frac{\text{Abs}(BC_m(j,k) - BC_o(j,k))}{\text{Min}(BC_m(j,k), BC_o(j,k))} \quad (3)$$

where  $j$  indexes latitude bins,  $k$  indexes altitude bins,  $nlat = 16$  is the total number of latitude bins (every 10 ° from 70 °S to 90 °N), and  $nalt = 10$  is the total number of altitude bins (every 1km from 0 to 10 km).  $\text{Abs}(BC_m(j,k) - BC_o(j,k))$  represents the absolute value of modeled BC minus observed BC averaged over the  $j^{\text{th}}$  and  $k^{\text{th}}$  latitude and altitude bin.  $N$  is the total number of latitude and altitude bins with recorded HIPPO observations. The model output daily averaged BC mixing ratios. For every record in HIPPO data (averaged in every 10s), we find modeled BC mixing ratio at the same longitude, latitude, altitude, and on the same day correspondingly. In this

way, modeled and observed BC mixing ratios are paired, and then are averaged respectively over latitude and altitude bins. We normalize the absolute errors by the minimum of observed and modeled BC so that  $MNMAE$  weights both high bias and low bias equally. Unlike the root mean square error, the  $MNMAE$  does not amplify the importance of the outliers.

Aging timescale affects atmospheric concentrations of BC through its influence on hygroscopicity and wet deposition of the particle. Thus,  $BC_m(j,k)$  and  $MNMAE$  are functions of aging timescale. We perform 13 simulations, each with different constant aging timescales (i.e. 4, 8, 12, 18, 24, 27.6, 38.4, 48, 60, 90, 120, 160 or 200 hours). Every simulation tags BC from each of 13 regions (i.e., North America, East Asia, Canada, ...); as mentioned in Section 2.3,  $BC_m(j,k) = \sum_r BC_m(j,k,r)$ , where  $r$  denotes each region. We construct  $BC_m(j,k)$  using all possible combinations of  $BC_m(j,k,r)$  from the 13 simulations. Then we check which combination of  $BC_m(j,k,r)$  best matches BC observations. Note that we constrain the aging rates of BC emitted from Africa, South America, and Australia to be the same since these three regions are all biomass burning dominated sources in the Southern Hemisphere, which effectively reduces the total number of tagged tracers from 13 to 11. Thus, we determine the best-fit BC aging timescale for each source region (out of  $13^{11}$  combinations in total) that minimizes  $MNAE$ .

~~Given the 13 simulations, each assuming a different aging timescale for BC (i.e. 4, 8, 12, 18, 24, 27.6, 38.4, 48, 60, 90, 120, 160, 200 hours), and the 13 tagged tracers for BC emissions from each source region, we determine the best-fit aging timescale for each source region by minimizing  $NMAE$ . Note that we assume the aging rates of BC emitted from Africa, South America, and Australia to be the same since these three regions are all biomass burning dominated sources in the Southern Hemisphere, effectively reducing the total number of tagged tracers from 13 to 11. Thus, we determine best fit BC aging timescale for each source region (out of  $13^{11}$  combinations in total) that minimizes  $NMAE$ .~~

### 3 Optimized BC profiles over the Pacific Ocean

To give a sense of the influence of aging timescale on BC, global BC burdens for the minimum and maximum aging timescales considered here (i.e. 4 and 200 hours) are shown in Figure 2. BC burden increases with aging timescale in both the lower (Figures 2d,e) and mid and upper troposphere (Figures 2a,b). For most regions, BC burden in remote areas and in the mid and upper troposphere is more sensitive to aging timescale than that in source regions and in the lower troposphere (Figure 2c,f). BC over the Pacific Ocean increases by a factor of 5-100 as the aging timescale increases from 4 to 200h (Figures 2c,f).

The dominant regional contributors to annual averaged BC burden for aging timescales of 4 and 200 hours are shown in Figure 3. Longer aging timescales increase the footprint areas dominated by the highest emitting source regions. For example, the area over the Pacific Ocean for which East Asian emissions dominate the burden is larger when aging timescale is 200 versus 4 h. Over source regions, BC in the lower troposphere is dominated by local emissions for both aging timescales. However, the dominant source of BC in the mid and upper troposphere over source regions can switch from local source emissions to long-range transport from other source regions when increasing aging timescale. For example, BC in the mid and upper troposphere over the United States is dominated by local emissions when aging timescale is 4 hours, but dominated by East Asian emissions when aging timescale is 200 hours. Thus, varying aging timescale can lead to substantial differences in BC simulation over the Pacific Ocean, supporting the need to constrain the aging timescale by observations.

~~Optimized aging timescales for each source region and season are shown in Table 1. Values differ significantly by source region and season. We find that the aging of BC from East Asia, North America, Southeast Asia and India is in most cases very fast (less than half a day). Optimized aging rate is relatively slow in the high-latitude regions (Canada, Europe and the former Soviet Union) in all seasons except summer (June July August, JJA), which can be explained by slower photochemistry in high latitudes under low sunlight in non-summer months.~~

~~The seasonality of aging timescales in the Arctic is consistent with Liu et al. (2011) who developed a parameterization for BC aging rate as a function of OH radical concentrations.~~

~~The optimized BC timescales reported here for East Asia and North America are consistent with observations in these regions, which show that BC is quickly mixed with hydrophilic species. Observations in an urban region of Japan find that the timescale for BC to become internally mixed is 12 hours, with coatings made of primarily sulfate and soluble organic carbon (Moteki et al., 2007). In Beijing and Mexico City, urban BC is observed to become internally mixed with sulfate in a few hours (Johnson et al., 2005; Cheng et al., 2012). Other studies show that biomass-burning aerosols tend to be internally mixed as emitted, and BC is often coated by soluble potassium salt (Li et al., 2003; Posfai et al., 2003). On the other hand, another modeling study finds that aerosols emitted by Southeast Asia experience a slower aging than aerosols emitted by East Asia (Shen et al., 2014). However, it is hard to judge which timescale is more reliable since there is no direct measurement on the timescale of hydrophobic BC converting to hydrophilic BC. More observations are needed to measure the hygroscopicity of BC-containing particles in different regions.~~

Optimized aging timescales for each source region and season are shown in Table 1. Ranges of plausible values for each optimized aging timescale based on perturbation simulations are also summarized in Table S1 in the supplementary materials. As shown in Table 1, values differ significantly by source region and season. The aging timescale of BC from East Asia, North America, India, and Southeast Asia is in most cases relatively short (i.e., less than half a day). The optimized BC timescales reported here for East Asia and North America are consistent with observations in these regions, which show that BC is quickly mixed with hydrophilic species. For instance, observations over an urban region of Japan find that the timescale for BC to become internally mixed is 12 hours, with coatings made of primarily sulfate and soluble organic carbon (Moteki et al., 2007). In Beijing and Mexico City, urban BC is observed to become internally mixed with sulfate in a few hours (Johnson et al., 2005; Cheng et al., 2012). Over Southeast Asia, BC emissions are mainly anthropogenic in origin (with a fast aging rate), except during spring



when large-scale biomass burning activities generate tremendous amounts of BC. The optimized springtime BC aging timescale for Southeast Asia is around 2 days, consistent with the findings of Shen et al. (2014). On the contrary, the optimized aging rate is relatively slow in the high-latitude regions (Canada, the former Soviet Union and in particular Europe) in all seasons except summer (June-July-August, JJA), which can be explained by slower photochemistry in high latitudes under low sunlight in non-summer months. Since measurements on BC aging timescale are scarce and limited to few places, more observations are needed to measure the hygroscopicity of BC-containing particles in different continents covering both source and downwind areas.

The seasonality of aging timescale reported here is largely consistent with Liu et al. (2011), who develop a parameterization for BC aging rate as a function of OH radical concentration. In this study, we further improve the parameterization of Liu et al. (2011) by finding best-fit values for constants that best match HIPPO observations with reference to our BC aging timescales. After conducting additional sensitivity simulations, we find that a set of parameters (i.e.,  $\beta=2.4 \times 10^{-11}$ , and  $\gamma=1 \times 10^{-6}$  in Equation (4) in Liu et al. (2011)) when employed in MOZART-4 can fit well the HIPPO observations as well as ground observations (see Figure S1 and S2 in supplementary material).

Figure 4 compares vertical profiles of BC simulated by the “improved model” and the “original model” with HIPPO observations in different latitude bands. Here, BC from the improved model is computed as the sum of tagged tracers corresponding to the optimized timescale for each region, whereas that from the original model uses the default configuration with aging timescale of 1.6 days. The vertical profiles of BC simulated by the improved model are much closer to the observations than the original model, which overestimates BC mass mixing ratios in nearly every campaign. In particular, values simulated by the improved model are near those for HIPPO2, 3 and 4 in both pattern and magnitude. *MNAE* is reduced significantly for each latitude band and HIPPO campaign, with reductions ranging from a factor of 2 to 25 (Figure 4).

Campaign-averaged *MNAE* is also reduced by a factor of 4-10 (Table 1). For comparison, we also

derive the ~~normalized~~-mean normalized bias (MNB) used in Samset et al. (2014). Values for the improved model are below 25% for every campaign (Table 1), lower than their reported ~~NMBMNB~~ for most AeroCom models. Figure S3 in the supplementary materials shows that the improved model also agrees with the surface air observations of BC in source regions over the United States, Europe and East Asia.

In a few cases, relatively large differences between the improved model and observations remain. These differences could be attributed to any number of factors (e.g., emissions, transport, cloud/precipitation, aging process, wet removal efficiency, etc.). For example, models could misrepresent BC wet deposition, originating from biases in precipitation. As shown in Figures S4 in the supplementary materials, though MOZART-4 generally captures well the spatial extent of precipitation during all HIPPO campaigns, biases occasionally appear when comparing to the NCEP reanalysis over the western Pacific. As another example, the model uses a monthly biomass burning emission inventory. This means that modeled emissions lack daily variation in biomass burning activities that could be important where biomass burning emissions dominate BC loading. Underestimates in BC mixing ratio may be partially due to abrupt emissions events that are not captured by the model. Lastly, since this study assumes that BC aging timescale in all the southern hemispheric continents is the same, we do not account for variability in BC aging rates from these regions that may exist in reality.

~~Differences between the improved model and observations remain in a few cases. Higher modeled versus observed BC in the tropics and in the northern mid-latitudes during HIPPO5 is likely due to the misrepresentation of clouds and precipitation in MOZART-4. As shown in Figures A1 and A2 (see the supplementary materials), precipitation predicted by MOZART-4 is generally less than NCEP reanalysis in the source regions of BC along the HIPPO5 trajectory (e.g. East Asia and Canada). Lower modeled versus observed BC in the Southern Hemisphere during HIPPO5 could stem from the fact that the model uses a monthly biomass burning emission inventory. This means that emissions lack daily variation in biomass burning activities that could~~

~~be important in reality where biomass burning emissions dominate BC loading. BC mass mixing ratios in the mid and upper troposphere over the South Pacific Ocean during HIPPO5 are higher than that during HIPPO1-4 by at least a factor of 2, implying that HIPPO5 might include abrupt emissions events that are not captured by the model.~~

#### 4 Regional contribution of source regions to BC loading

Seasonally varying optimized aging timescales for each source region are used to investigate the dominant source regions contributing to zonal mean mass mixing ratio of BC over the Pacific Ocean (130°W-160°E) (Figure 5a), and column burden of BC around the globe (Figure 5b). We assume that optimized aging timescales for HIPPO1,2,3 and 4 are representative for DJF, SON, MAM, and JJA, respectively (see Table 1). BC in the lower troposphere over the Pacific Ocean is mostly controlled by either emissions from RR (“rest regions”, i.e. ships), or the closest upwind source regions like Australia, South America and East Asia (Figure 5a). On the other hand, BC in the mid and upper troposphere is influenced mostly by BC emissions from major source regions: East Asia, Australia, South America, Africa, and North America. East Asian BC emissions, which are mainly of anthropogenic origin, dominate BC loading over the Northern Pacific Ocean even though its aging is fast. Also, as shown in Figure 5b, the Arctic BC is dominated by European emissions, while BC in the Antarctica is dominated by South American emissions.

The relative contribution of emissions from each source region to BC burden over each receptor region is presented in Table 2. We add an extra receptor region, the central Pacific Ocean (PO), defined as 60°S-58°N, 160°E-130°W. In the central Pacific OceanPO, the dominant contributor is East Asia, accounting for 26% of the burden. In the former Soviet Union, middle Asia, and Canada, local emissions account for no more than 50% of the BC burden, whereas Europe contributes 44%, 43%, and 14% to their burdens, respectively. BC over other regions is dominated by local sources. For example, local sources are responsible for 89%, 77%, and 73%

of the BC burden in India, East Asia and North America. Thus, controlling local anthropogenic sources is expected to have the largest impact on BC burdens in these regions.

Table 3 compares the annual mean (2009-2011 average) dry deposition flux, wet deposition flux, burden, and lifetime for BC emitted from different source regions. The lifetime of BC estimated by the improved model is 4.9 days. This lifetime is quite similar to that from recent studies (Wang et al. (2014) and Hodnebrog et al. (2014)). They modify model scavenging processes to better reproduce HIPPO observations, and find that BC lifetimes are shortened from 5.9 to 4.2 days, and from 6.3 to 3.9 days, respectively. In addition, Samset et al. (2014) find that while the lifetime of BC is  $6.8 \pm 1.8$  days averaged over 13 AeroCom models, the models with lifetime less than 5 days best match HIPPO observations. Our result is in accordance with their conclusions, and is lower than the BC lifetime of 6.1 days estimated by Bond et al. (2013).

Table 3 also shows that the lifetime of BC varies significantly by source region, ranging from 2 to 10 days. Regional variation in the lifetime of BC is likely caused by differences in wet scavenging, which depends on precipitation patterns and the hygroscopicity of BC-containing particles. The lifetimes of BC emitted from the former Soviet Union (4.4 days), East Asia (2.2 days), North America (3.7 days) and Southeast Asia (3.1 days) are shorter than the corresponding global average. Given the wide range of BC lifetime by source region, the relative contribution of different regions to burdens is not well characterized by the relative rates of emissions. For example, although East Asia emits the largest amount of BC, its lifetime is the shortest (~2 days). This means that the contribution of East Asian emissions to the global BC burden is only 1/3 of that of the second-leading source region (Africa). Using a different model and a rough division of source regions, Wang et al. (2014) also find that the lifetimes of East Asian (2.8 days), Southeast Asian (2.1 days), and American BC emissions (3.0 days) are shorter than the global average lifetime (4.7 days).

## 5 Dependence of BC lifetime on aging timescale

In this section, we further investigate the dependence of lifetime (derived by the annual mean burden and removal flux) on aging timescale for BC emitted from different source regions. As shown in Figure 6, the lifetime of BC originating from different regions increases approximately linearly with aging timescale. Although there is variation in the y-intercepts for curves of lifetime versus aging timescale, slopes are quite similar. In an effort to understand the drivers of the relationship between lifetime  $T$  (hr) and aging timescale  $\tau$  (hr), we derive a theoretical description here. Taking the global atmosphere as a box, the mass balance for  $B_1$  (annual mean hydrophobic BC burden, units of kg) and  $B_2$  (annual mean hydrophilic BC burden, units of kg) are

$$\frac{dB_1}{dt} = (1 - \alpha)E - \frac{B_1}{\tau} - K_D B_1 \quad (4)$$

$$\frac{dB_2}{dt} = \alpha E + \frac{B_1}{\tau} - (K_D + K_W)B_2 \quad (5)$$

where  $\alpha$  is the fraction of BC emitted that is hydrophilic,  $E$  ( $\text{kg hr}^{-1}$ ) is the annual mean emission rate, and  $K_D$  and  $K_W$  are the first-order dry and wet deposition coefficients ( $\text{hr}^{-1}$ ), respectively.  $K_W$  accounts for both precipitation intensity and scavenging efficiency.

Assuming that both hydrophilic and hydrophobic BC is in steady state, we derive the lifetime of BC as:

$$T = \frac{B_1 + B_2}{E} = \frac{((1-\alpha)K_W + K_D)\tau + 1}{(1 + K_D\tau)(K_D + K_W)} \quad (6)$$

If further assuming that  $K_D$  and  $K_W$  are not dependent on  $\tau$ , we then derive the slope  $S$  (Equation 7) and intercept (Equation 8) of the  $T$ - $\tau$  curve:

$$S = \frac{dT}{d\tau} = \frac{(1-\alpha)K_W}{(K_D + K_W)(1 + K_D\tau)^2} \quad (7)$$

$$T(\tau=0) = \frac{1}{K_W + K_D} \quad (8)$$

The slope  $\left(\frac{dT}{d\tau}\right)S$  represents the sensitivity of BC lifetime to aging timescale, which is a function of wet and dry deposition coefficients of BC, and the fraction of BC emitted that is hydrophilic.

Given Equation 7, if  $\alpha = 1$  then  $\frac{dT}{d\tau}S = 0$ , implying that all BC is aged and therefore hydrophilic as emitted. If  $K_D = 0$  then  $\frac{dT}{d\tau}S = 1 - \alpha$ . Therefore, if  $K_D$  is negligible, the lifetime of BC will be linearly related to aging timescale. In addition, lower fractions of hydrophilic BC in emissions ( $\alpha$ ) will lead to larger sensitivities of BC lifetime to aging timescale  $\left(\frac{dT}{d\tau}S\right)$ . In

MOZART-4,  $\alpha$  is assumed to be 0.2 for all emission sources. So if  $K_D$  is negligible, the theoretical slope of the T- $\tau$  curve is  $1-0.2=0.8$ , which is very close to the curve for untagged BC (black line) in Figure 6.

The intercepts of T- $\tau$  curves represent the lifetime of BC when the aging process is extremely fast (i.e. low values of aging timescale) such that all emitted BC can be regarded to be hydrophilic. As shown by equation 8, the intercept is a function of local wet deposition coefficient and dry deposition coefficient. Intercepts of the T- $\tau$  curves vary by source, ranging from 40 to 170 hours. BC emitted in the Middle East, Africa, Canada, Australia, and South America has a larger intercept than the untagged BC because the climate in these regions lacks precipitation. The Middle East is dry and lacks precipitation in general, and emissions from Africa, Canada, and Australia are mainly from biomass burning activities that usually occur during their dry seasons.

It should be noted that in our derivation of Eqs. (7) and (8), we assume that  $K_D$  and  $K_W$  are independent of  $\tau$ . In reality, however,  $K_D$  and  $K_W$  can depend on  $\tau$ . For example, as aging timescale increases, BC has a longer lifetime and is more likely to encounter precipitation in regions farther away from the source. Nonetheless, the discussion above helps elucidate that the dependence of lifetime on aging timescale is determined by the fraction of emitted BC that is hydrophilic, and the factors that influence dry and wet deposition (e.g. precipitation).

Since the aging timescale varies by region and season, the common practice in modeling of setting a fixed global uniform aging rate may lead to significant misrepresentation of BC lifetime and burden. Employing realistic aging timescales is especially important for regions shown in Figure 6 with the highest slopes and lowest intercepts; changes in aging timescale would lead to the largest relative changes in BC lifetime in these regions. For instance, for Southeast Asia, increasing the aging timescale of BC from 0 to 60 hours nearly doubles its lifetime.

Policies that control SO<sub>2</sub> and other soluble compounds may slow BC aging, increase the lifetime of BC, and partially offset efforts made on BC mitigation. For example, as indicated by a chamber study, employing after-treatment technologies such as oxidation catalysts in combustion systems can reduce emissions of volatile organic compounds and formation of secondary organic aerosols (SOA) that could internally mix with BC, ultimately slowing the aging of BC (Tritscher et al., 2011). Thus, policies for protecting human health that target reductions in emissions of only fine soluble particulate matter (i.e., sulfate, nitrate and SOA) could increase BC burden through increases in aging timescale, and potentially enhances its positive radiative forcing.

## 6 Caveats

We note that there are multiple limitations to our approach. Firstly, we assume that model parameterizations of wet and dry deposition, precipitation, transport, and emissions are realistic, even though these processes also affect BC distributions and have uncertainties (Vignati et al., 2010; Fan et al., 2012). Consequently, the optimized aging timescales may partially counter biases in these processes (i.e. other than aging), and may vary according to the model used. For example, as model resolution increases, aerosol-cloud interactions in climate models can be better resolved, which can improve the simulation of BC transport (Ma et al., 2013; Ma et al., 2014). Therefore, the optimized aging timescales might change if models with different cloud schemes or spatial resolutions are used. Secondly, due to limitations in computing resources, we carry out simulations assuming 13 discrete values for aging timescale. Optimized aging timescale could



have been more precisely determined with more simulations. Thirdly, the optimized aging results may somewhat depend on the error matrix chosen. We conduct additional simulations with different error matrices (see Table S2, S3 in supplementary material). The results are overall similar, but in some cases moderate differences are found. Fourthly, the computed optimized aging rate is more accurate for tracers (i.e. source regions) with larger emissions and in closer proximity to the Pacific Ocean (e.g. East Asia). This is because modeled BC concentrations over the Pacific (i.e. the location of HIPPO observations) for each latitude and longitude bin are typically dominated by only a few source regions, and the sensitivity of MNAE on each regional BC tracer is different (see Figure S5 in the supplementary material). For some source regions, observations in other remote regions would provide a better constraint for optimizing aging timescale in the model. More specifically, aircraft observations over the Atlantic Ocean could better constrain aging timescales for BC emitted from Africa and South America. As new observations become available, this study could be repeated to more accurately optimize the aging timescale for source regions with lower relative contributions to BC over the Pacific (e.g. Middle Asia). The goal of the optimization presented here is not to provide precise aging timescales that can be directly used in models, since models differ significantly in their parameterizations of physical and chemical processes, particularly the wet scavenging. Also, BC aging includes complicated chemistry and physics, but is simplified in our modeling as a first-order conversion from hydrophobic to hydrophilic BC. Nevertheless, this study proposes a useful method to utilize all HIPPO observations and explore the spatiotemporal pattern of BC aging timescales globally.

~~We note that there are limitations to our approach. First, we assume that model parameterizations of wet and dry deposition, transport, and emissions are realistic, even though these processes also affect BC distributions and include uncertainties (Vignati et al., 2010; Fan et al., 2012). Consequently, the optimized aging timescales may partially counter biases in these processes (i.e. other than aging), and may vary according to the model used. Also, only HIPPO is used in our study. For some source regions, observations in other remote regions would provide a better~~

~~constraint for optimizing aging timescale in the model. More specifically, aircraft observations over the Atlantic Ocean could better constrain aging timescales for BC emitted from Africa and South America. As new observations become available, this study could be repeated to optimize the aging timescale for all source regions. BC aging includes complicated chemistry and physics, and is simplified in our modeling as a first-order conversion from hydrophobic to hydrophilic BC. Nevertheless, the goal of our aging optimization is not to provide an aging timescale that can be directly used in models (since models differ significantly in parameterizing wet scavenging efficiency), but to estimate the spatiotemporal pattern of aging timescales globally using every HIPPO observation.~~

## 7 Conclusions

In this study, we tag BC emitted from thirteen regions around the globe, and conduct a set of sensitivity simulations to investigate how different aging timescales affect spatial distributions and source-receptor relationships for BC in a global chemical transport model, MOZART-4. We find that BC burden and source-receptor relationships are remarkably sensitive to the assumed aging timescale in the model; this motivates our use of HIPPO observations to optimize BC aging timescale by minimizing model-measurement differences. Physically-based dry and wet deposition schemes and optimized aging timescales for different regions are employed in MOZART-4, which significantly improves the model's performance over the Pacific Ocean relative to the default model; the campaign-averaged ~~normalized~~ mean normalized absolute error is reduced by a factor of 4-10. The optimized aging timescales vary greatly by source region and season. In the Northern Hemisphere, we find that the aging timescale for BC emitted in mid- and low-latitude locations is in general less than half a day, whereas that for BC emitted from high-latitude locations in most seasons (i.e. Spring, Fall, and Winter) is 4-8 days.

Using the improved model, we find that the dominant contributors to BC in the lower troposphere over the central Pacific Ocean are local sources (i.e. ship emissions), Australia, South America

and East Asia. For the mid and upper troposphere over the Pacific Ocean, the dominant sources are East Asia, Australia, South America, Africa, and North America. East Asian emissions contribute the most (26%) to the total burden of tropospheric BC over the Pacific Ocean. We also find that BC emitted from different source regions has distinct atmospheric lifetimes, suggesting that comparing only emissions of different regions does not directly predict their contribution to burden and therefore climate consequences. The lifetimes of BC emitted from East Asia, Southeast Asia, North America, and the former Soviet Union are 2.2, 3.2, 3.8, and 4.4 days respectively, shorter than 4.9 days, the global average lifetime.

Using model sensitivity simulations we determine the sensitivity of BC lifetime to aging timescale for emissions from each source region. The lifetime-aging timescale relationship is for most regions nearly linear. The sensitivity is influenced by wet and dry deposition rates, and more importantly by a parameter that describes the fraction of BC emissions that are emitted directly as hydrophilic.

Future observations that speciate coatings on BC and measure hygroscopicity of both freshly emitted and aged BC in different regions and seasons are needed to further constrain aging timescales and understand the physics and chemistry of the aging process. The lifetime of BC determines its global reach, and consequently its radiative forcing on the climate system. BC with slow aging timescales and long lifetimes can influence the climate in remote areas substantially (e.g. over the oceans and the Arctic). In principle, the estimated climate impacts of BC emitted from different regions rely on the representation of particles' hygroscopicity and the assumptions on aging timescales. Our study highlights the importance of accurately representing aging processes in models and parameterizing aging timescales differently in different regions and seasons.

We recommend that future inter-model comparisons like AeroCom use tagging techniques to compare model estimates of the lifetimes of BC emitted from different regions. The tracer tagging technique utilized here can also be used to estimate regional source contributions to BC

observed in future aircraft campaigns, to help choose locations for future campaigns, and to attribute discrepancies in inter-model comparisons to specific source regions.

## **Acknowledgements**

We thank Xiaoyuan Li, Cenlin He, Wei Tao, Jing Meng, Huizhong Shen, Maowei Wu, Zhaoyi Shen, Kan Chen and Yan Xia for their helpful contributions and suggestions to this study. We also thank Huisheng Bian and other three reviewers for their constructive comments and suggestions. This work was supported by funding from the National Natural Science Foundation of China under awards 41222011, 41390241 and 41130754, the Research Project of the Chinese Ministry of Education No. 113001A, the undergraduate student research training program, and the 111 Project (B14001).

## **References**

- Ban-Weiss, G. A., Cao, L., Bala, G., and Caldeira, K.: Dependence of climate forcing and response on the altitude of black carbon aerosols, *Clim Dynam*, 38, 897-911, DOI 10.1007/s00382-011-1052-y, 2012.
- Bell, M. L., Ebisu, K., Peng, R. D., Samet, J. M., and Dominici, F.: Hospital Admissions and Chemical Composition of Fine Particle Air Pollution, *Am J Resp Crit Care*, 179, 1115-1120, DOI 10.1164/rccm.200808-1240OC, 2009.
- Bian, H., Colarco, P. R., Chin, M., Chen, G., Rodriguez, J. M., Liang, Q., Blake, D., Chu, D. A., da Silva, A., Darmenov, A. S., Diskin, G., Fuelberg, H. E., Huey, G., Kondo, Y., Nielsen, J. E., Pan, X., and Wisthaler, A.: Source attributions of pollution to the Western Arctic during the NASA ARCTAS field campaign, *Atmospheric Chemistry and Physics*, 13, 4707-4721, DOI 10.5194/acp-13-4707-2013, 2013.
- Bollasina, M. A., Ming, Y., and Ramaswamy, V.: Anthropogenic Aerosols and the Weakening of the South Asian Summer Monsoon, *Science*, 334, 502-505, DOI 10.1126/science.1204994, 2011.

Bollasina, M. A., Ming, Y., Ramaswamy, V., Schwarzkopf, M. D., and Naik, V.: Contribution of local and remote anthropogenic aerosols to the twentieth century weakening of the South Asian Monsoon, *Geophysical Research Letters*, 41, 680-687, Doi 10.1002/2013gl058183, 2014.

Bond, T. C., Doherty, S. J., Fahey, D. W., Forster, P. M., Berntsen, T., DeAngelo, B. J., Flanner, M. G., Ghan, S., Karcher, B., Koch, D., Kinne, S., Kondo, Y., Quinn, P. K., Sarofim, M. C., Schultz, M. G., Schulz, M., Venkataraman, C., Zhang, H., Zhang, S., Bellouin, N., Guttikunda, S. K., Hopke, P. K., Jacobson, M. Z., Kaiser, J. W., Klimont, Z., Lohmann, U., Schwarz, J. P., Shindell, D., Storelvmo, T., Warren, S. G., and Zender, C. S.: Bounding the role of black carbon in the climate system: A scientific assessment, *Journal of Geophysical Research-Atmospheres*, 118, 5380-5552, Doi 10.1002/Jgrd.50171, 2013.

Bourgeois, Q., and Bey, I.: Pollution transport efficiency toward the Arctic: Sensitivity to aerosol scavenging and source regions, *J. Geophys. Res.*, 116, D08213, 10.1029/2010jd015096, 2011.

China, S., Scarnato, B., Owen, R. C., Zhang, B., Ampadu, M. T., Kumar, S., Dzepina, K., Dziobak, M. P., Fialho, P., Perlinger, J. A., Hueber, J., Helmig, D., Mazzoleni, L. R., and Mazzoleni, C.: Morphology and mixing state of aged soot particles at a remote marine free troposphere site: Implications for optical properties, *Geophysical Research Letters*, 42, 2014GL062404, 10.1002/2014gl062404, 2015.

Cozic, J., Verheggen, B., Mertes, S., Connolly, P., Bower, K., Petzold, A., Baltensperger, U., and Weingartner, E.: Scavenging of black carbon in mixed phase clouds at the high alpine site Jungfraujoch, *Atmospheric Chemistry and Physics*, 7, 1797-1807, 2007.

Croft, B., Pierce, J. R., Martin, R. V., Hoose, C., and Lohmann, U.: Uncertainty associated with convective wet removal of entrained aerosols in a global climate model, *Atmospheric Chemistry and Physics*, 12, 10725-10748, DOI 10.5194/acp-12-10725-2012, 2012.

Croft, B., Lohmann, U., Martin, R. V., Stier, P., Wurzler, S., Feichter, J., Hoose, C., Heikkila, U., van Donkelaar, A., and Ferrachat, S.: Influences of in-cloud aerosol scavenging parameterizations on aerosol concentrations and wet deposition in ECHAM5-HAM, *Atmospheric Chemistry and Physics*, 10, 1511-1543, 2010.

Emmons, L. K., Walters, S., Hess, P. G., Lamarque, J. F., Pfister, G. G., Fillmore, D., Granier, C., Guenther, A., Kinnison, D., Laepple, T., Orlando, J., Tie, X., Tyndall, G., Wiedinmyer, C., Baughcum, S. L., and Kloster, S.: Description and evaluation of the Model for Ozone and Related chemical Tracers, version 4 (MOZART-4), *Geosci. Model Dev.*, 3, 43-67, 2010.

Evan, A. T., Kossin, J. P., Chung, C., and Ramanathan, V.: Arabian Sea tropical cyclones intensified by emissions of black carbon and other aerosols, *Nature*, 479, 94-U119, Doi 10.1038/Nature10552, 2011.

Fan, S. M., Schwarz, J. P., Liu, J., Fahey, D. W., Ginoux, P., Horowitz, L. W., Levy, H., Ming, Y., and Spackman, J. R.: Inferring ice formation processes from global-scale black carbon profiles observed in the remote atmosphere and model simulations, *Journal of Geophysical Research-Atmospheres*, 117, Artn D23205 Doi 10.1029/2012jd018126, 2012.

Feng, H.: A 3-mode parameterization of below-cloud scavenging of aerosols for use in atmospheric dispersion models, *Atmos Environ*, 41, 6808-6822, DOI 10.1016/j.atmosenv.2007.04.046, 2007.

Flanner, M. G., Zender, C. S., Randerson, J. T., and Rasch, P. J.: Present-day climate forcing and response from black carbon in snow, *Journal of Geophysical Research-Atmospheres*, 112, Artn D11202 Doi 10.1029/2006jd008003, 2007.

Gallagher, M. W., Nemitz, E., Dorsey, J. R., Fowler, D., Sutton, M. A., Flynn, M., and Duyzer, J.: Measurements and parameterizations of small aerosol deposition velocities to grassland, arable crops, and forest: Influence of surface roughness length on deposition, *Journal of Geophysical Research-Atmospheres*, 107, Artn 4154 Doi 10.1029/2001jd000817, 2002.

Hack, J. J.: Parameterization of moist convection in the National Center for Atmospheric Research community climate model (CCM2), *Journal of Geophysical Research-Atmospheres*, 99, 5551-5568, Doi 10.1029/93jd03478, 1994.

Hansen, J., and Nazarenko, L.: Soot climate forcing via snow and ice albedos, *P Natl Acad Sci USA*, 101, 423-428, DOI 10.1073/pnas.2237157100, 2004.

He, C. L., Li, Q. B., Liou, K. N., Takano, Y., Gu, Y., Qi, L., Mao, Y. H., and Leung, L. R.: Black carbon radiative forcing over the Tibetan Plateau, *Geophysical Research Letters*, 41, 7806-7813, Doi 10.1002/2014gl062191, 2014.

Hodnebrog, O., Myhre, G., and Samset, B. H.: How shorter black carbon lifetime alters its climate effect, *Nat Commun*, 5, Artn 5065 Doi 10.1038/Ncomms6065, 2014.

Holtslag, A. A. M., and Boville, B. A.: Local Versus Nonlocal Boundary-Layer Diffusion in a Global Climate Model, *J Climate*, 6, 1825-1842, Doi 10.1175/1520-0442(1993)006<1825:Lvnbl>2.0.Co;2, 1993.

Horowitz, L. W., Walters, S., Mauzerall, D. L., Emmons, L. K., Rasch, P. J., Granier, C., Tie, X. X., Lamarque, J. F., Schultz, M. G., Tyndall, G. S., Orlando, J. J., and Brasseur, G. P.: A global simulation of tropospheric ozone and related tracers: Description and evaluation of MOZART, version 2, *Journal of Geophysical Research-Atmospheres*, 108, Artn 4784 Doi 10.1029/2002jd002853, 2003.

Huang, Y., Wu, S., Dubey, M. K., and French, N. H. F.: Impact of aging mechanism on model simulated carbonaceous aerosols, *Atmospheric Chemistry and Physics*, 13, 6329-6343, DOI 10.5194/acp-13-6329-2013, 2013.

Janssen, N. A. H., Hoek, G., Simic-Lawson, M., Fischer, P., van Bree, L., ten Brink, H., Keuken, M., Atkinson, R. W., Anderson, H. R., Brunekreef, B., and Cassee, F. R.: Black Carbon as an Additional Indicator of the Adverse Health Effects of Airborne Particles Compared with PM10 and PM2.5, *Environ Health Persp*, 119, 1691-1699, Doi 10.1289/Ehp.1003369, 2011.

Kaneyasu, N., and Murayama, S.: High concentrations of black carbon over middle latitudes in the North Pacific Ocean, *Journal of Geophysical Research-Atmospheres*, 105, 19881-19890, 2000.

Kipling, Z., Stier, P., Schwarz, J. P., Perring, A. E., Spackman, J. R., Mann, G. W., Johnson, C. E., and Telford, P. J.: Constraints on aerosol processes in climate models from vertically-resolved

aircraft observations of black carbon, *Atmospheric Chemistry and Physics*, 13, 5969-5986, DOI 10.5194/acp-13-5969-2013, 2013.

Koch, D., and Hansen, J.: Distant origins of Arctic black carbon: A Goddard Institute for Space Studies ModelE experiment, *Journal of Geophysical Research-Atmospheres*, 110, Artn D04204 Doi 10.1029/2004jd005296, 2005.

Koch, D., and Del Genio, A. D.: Black carbon semi-direct effects on cloud cover: review and synthesis, *Atmospheric Chemistry and Physics*, 10, 7685-7696, DOI 10.5194/acp-10-7685-2010, 2010.

Koch, D., Schulz, M., Kinne, S., McNaughton, C., Spackman, J. R., Balkanski, Y., Bauer, S., Berntsen, T., Bond, T. C., Boucher, O., Chin, M., Clarke, A., De Luca, N., Dentener, F., Diehl, T., Dubovik, O., Easter, R., Fahey, D. W., Feichter, J., Fillmore, D., Freitag, S., Ghan, S., Ginoux, P., Gong, S., Horowitz, L., Iversen, T., Kirkevåg, A., Klimont, Z., Kondo, Y., Krol, M., Liu, X., Miller, R., Montanaro, V., Moteki, N., Myhre, G., Penner, J. E., Perlwitz, J., Pitari, G., Reddy, S., Sahu, L., Sakamoto, H., Schuster, G., Schwarz, J. P., Seland, O., Stier, P., Takegawa, N., Takemura, T., Textor, C., van Aardenne, J. A., and Zhao, Y.: Evaluation of black carbon estimations in global aerosol models, *Atmospheric Chemistry and Physics*, 9, 9001-9026, 2009.

Kotzick, R., and Niessner, R.: The effects of aging processes on critical supersaturation ratios of ultrafine carbon aerosols, *Atmos Environ*, 33, 2669-2677, Doi 10.1016/S1352-2310(98)00315-X, 1999.

Kotzick, R., Panne, U., and Niessner, R.: Changes in condensation properties of ultrafine carbon particles subjected to oxidation by ozone, *J Aerosol Sci*, 28, 725-735, Doi 10.1016/S0021-8502(96)00471-5, 1997.

Laborde, M., Crippa, M., Tritscher, T., Juranyi, Z., Decarlo, P. F., Temime-Roussel, B., Marchand, N., Eckhardt, S., Stohl, A., Baltensperger, U., Prevot, A. S. H., Weingartner, E., and Gysel, M.: Black carbon physical properties and mixing state in the European megacity Paris, *Atmospheric Chemistry and Physics*, 13, 5831-5856, DOI 10.5194/acp-13-5831-2013, 2013.



Lamarque, J. F., Bond, T. C., Eyring, V., Granier, C., Heil, A., Klimont, Z., Lee, D., Liousse, C., Mieville, A., Owen, B., Schultz, M. G., Shindell, D., Smith, S. J., Stehfest, E., Van Aardenne, J., Cooper, O. R., Kainuma, M., Mahowald, N., McConnell, J. R., Naik, V., Riahi, K., and van Vuuren, D. P.: Historical (1850-2000) gridded anthropogenic and biomass burning emissions of reactive gases and aerosols: methodology and application, *Atmospheric Chemistry and Physics*, 10, 7017-7039, DOI 10.5194/acp-10-7017-2010, 2010.

Lammel, G., and Novakov, T.: Water Nucleation Properties of Carbon-Black and Diesel Soot Particles, *Atmos Environ*, 29, 813-823, Doi 10.1016/1352-2310(94)00308-8, 1995.

Lau, N. C., and Nath, M. J.: A Model Study of the Air-Sea Interaction Associated with the Climatological Aspects and Interannual Variability of the South Asian Summer Monsoon Development, *J Climate*, 25, 839-857, Doi 10.1175/Jcli-D-11-00035.1, 2012.

Lin, S. J., and Rood, R. B.: Multidimensional flux-form semi-Lagrangian transport schemes, *Mon Weather Rev*, 124, 2046-2070, Doi 10.1175/1520-0493(1996)124<2046:Mffslt>2.0.Co;2, 1996.

Liu, D., Allan, J., Whitehead, J., Young, D., Flynn, M., Coe, H., McFiggans, G., Fleming, Z. L., and Bandy, B.: Ambient black carbon particle hygroscopic properties controlled by mixing state and composition, *Atmospheric Chemistry and Physics*, 13, 2015-2029, DOI 10.5194/acp-13-2015-2013, 2013a.

Liu, J. F., Fan, S. M., Horowitz, L. W., and Levy, H.: Evaluation of factors controlling long-range transport of black carbon to the Arctic, *Journal of Geophysical Research-Atmospheres*, 116, Artn D04307 Doi 10.1029/2010jd015145, 2011.

Liu, Y. K., Liu, J. F., and Tao, S.: Interannual variability of summertime aerosol optical depth over East Asia during 2000-2011: a potential influence from El Nino Southern Oscillation, *Environ Res Lett*, 8, Artn 044034 Doi 10.1088/1748-9326/8/4/044034, 2013b.

Ma, P.-L., Gattiker, J. R., Liu, X., and Rasch, P. J.: A novel approach for determining source-receptor relationships in model simulations: a case study of black carbon transport in northern hemisphere winter, *Environ Res Lett*, 8, 024042, Artn 024042 Doi 10.1088/1748-9326/8/2/024042, 2013a.

Ma, P. L., Rasch, P. J., Fast, J. D., Easter, R. C., Gustafson, W. I., Liu, X., Ghan, S. J., and Singh, B.: Assessing the CAM5 physics suite in the WRF-Chem model: implementation, resolution sensitivity, and a first evaluation for a regional case study, *Geosci. Model Dev.*, 7, 755-778, 10.5194/gmd-7-755-2014, 2014.

Ma, P. L., Rasch, P. J., Wang, H. L., Zhang, K., Easter, R. C., Tilmes, S., Fast, J. D., Liu, X. H., Yoon, J. H., and Lamarque, J. F.: The role of circulation features on black carbon transport into the Arctic in the Community Atmosphere Model version 5 (CAM5), *Journal of Geophysical Research-Atmospheres*, 118, 4657-4669, 10.1002/jgrd.50411, 2013b.

Matsui, H., and Koike, M.: New source and process apportionment method using a three-dimensional chemical transport model: Process, Age, and Source region Chasing ALgorithm (PASCAL), *Atmos Environ*, 55, 399-409, DOI 10.1016/j.atmosenv.2012.02.080, 2012.

McMeeking, G. R., Good, N., Petters, M. D., McFiggans, G., and Coe, H.: Influences on the fraction of hydrophobic and hydrophilic black carbon in the atmosphere, *Atmospheric Chemistry and Physics*, 11, 5099-5112, DOI 10.5194/acp-11-5099-2011, 2011.

Ming, Y., Ramaswamy, V., and Persad, G.: Two opposing effects of absorbing aerosols on global-mean precipitation, *Geophysical Research Letters*, 37, Artn L13701 Doi 10.1029/2010gl042895, 2010.

Moteki, N., Kondo, Y., Miyazaki, Y., Takegawa, N., Komazaki, Y., Kurata, G., Shirai, T., Blake, D. R., Miyakawa, T., and Koike, M.: Evolution of mixing state of black carbon particles: Aircraft measurements over the western Pacific in March 2004, *Geophysical Research Letters*, 34, Artn L11803 Doi 10.1029/2006gl028943, 2007.

Oshima, N., and Koike, M.: Development of a parameterization of black carbon aging for use in general circulation models, *Geosci. Model Dev.*, 6, 263-282, DOI 10.5194/gmd-6-263-2013, 2013.

Ramanathan, V., and Carmichael, G.: Global and regional climate changes due to black carbon, *Nat. Geosci.*, 1, 221-227, 10.1038/ngeo156, 2008.

Rasch, P. J., Mahowald, N. M., and Eaton, B. E.: Representations of transport, convection, and the hydrologic cycle in chemical transport models: Implications for the modeling of short-lived and soluble species, *Journal of Geophysical Research-Atmospheres*, 102, 28127-28138, Doi 10.1029/97jd02087, 1997.

Rasch, P. J., Barth, M. C., Kiehl, J. T., Schwartz, S. E., and Benkovitz, C. M.: A description of the global sulfur cycle and its controlling processes in the National Center for Atmospheric Research Community Climate Model, Version 3, *Journal of Geophysical Research-Atmospheres*, 105, 1367-1385, Doi 10.1029/1999jd900777, 2000.

Riemer, N., Vogel, H., and Vogel, B.: Soot aging time scales in polluted regions during day and night, *Atmospheric Chemistry and Physics*, 4, 1885-1893, 2004.

Riemer, N., West, M., Zaveri, R., and Easter, R.: Estimating black carbon aging time-scales with a particle-resolved aerosol model, *J Aerosol Sci*, 41, 143-158, DOI 10.1016/j.jaerosci.2009.08.009, 2010.

Saikawa, E., Naik, V., Horowitz, L. W., Liu, J. F., and Mauzerall, D. L.: Present and potential future contributions of sulfate, black and organic carbon aerosols from China to global air quality, premature mortality and, radiative forcing, *Atmos Environ*, 43, 2814-2822, DOI 10.1016/j.atmosenv.2009.02.017, 2009.

Samset, B., Myhre, G., Herber, A., Kondo, Y., Li, S.-M., Moteki, N., Koike, M., Oshima, N., Schwarz, J., and Balkanski, Y.: Modeled black carbon radiative forcing and atmospheric lifetime in AeroCom Phase II constrained by aircraft observations, *Atmospheric Chemistry and Physics*, 14, 20083-20115, 2014.

Samset, B. H., and Myhre, G.: Vertical dependence of black carbon, sulphate and biomass burning aerosol radiative forcing, *Geophysical Research Letters*, 38, Artn L24802 Doi 10.1029/2011gl049697, 2011.

Samset, B. H., and Myhre, G.: Climate response to externally mixed black carbon as a function of altitude, *Journal of Geophysical Research: Atmospheres*, 2014JD022849, 10.1002/2014jd022849, 2015.

Samset, B. H., Myhre, G., Schulz, M., Balkanski, Y., Bauer, S., Berntsen, T. K., Bian, H., Bellouin, N., Diehl, T., Easter, R. C., Ghan, S. J., Iversen, T., Kinne, S., Kirkevåg, A., Lamarque, J. F., Lin, G., Liu, X., Penner, J. E., Seland, O., Skeie, R. B., Stier, P., Takemura, T., Tsigaridis, K., and Zhang, K.: Black carbon vertical profiles strongly affect its radiative forcing uncertainty, *Atmospheric Chemistry and Physics*, 13, 2423-2434, DOI 10.5194/acp-13-2423-2013, 2013.

Satheesh, S. K.: Aerosol radiative forcing over land: effect of surface and cloud reflection, *Ann Geophys-Germany*, 20, 2105-2109, 2002.

Schwarz, J. P., Spackman, J. R., Gao, R. S., Watts, L. A., Stier, P., Schulz, M., Davis, S. M., Wofsy, S. C., and Fahey, D. W.: Global-scale black carbon profiles observed in the remote atmosphere and compared to models, *Geophysical Research Letters*, 37, Artn L18812 Doi 10.1029/2010gl044372, 2010.

Schwarz, J. P., Samset, B. H., Perring, A. E., Spackman, J. R., Gao, R. S., Stier, P., Schulz, M., Moore, F. L., Ray, E. A., and Fahey, D. W.: Global-scale seasonally resolved black carbon vertical profiles over the Pacific, *Geophysical Research Letters*, 40, 2013GL057775, 10.1002/2013gl057775, 2013.

Schwarz, J. P., Spackman, J. R., Fahey, D. W., Gao, R. S., Lohmann, U., Stier, P., Watts, L. A., Thomson, D. S., Lack, D. A., Pfister, L., Mahoney, M. J., Baumgardner, D., Wilson, J. C., and Reeves, J. M.: Coatings and their enhancement of black carbon light absorption in the tropical atmosphere, *Journal of Geophysical Research-Atmospheres*, 113, Artn D03203 Doi 10.1029/2007jd009042, 2008.

Schwarz, J. P., Gao, R. S., Fahey, D. W., Thomson, D. S., Watts, L. A., Wilson, J. C., Reeves, J. M., Darbeheshti, M., Baumgardner, D. G., Kok, G. L., Chung, S. H., Schulz, M., Hendricks, J., Lauer, A., Karcher, B., Slowik, J. G., Rosenlof, K. H., Thompson, T. L., Langford, A. O., Loewenstein, M., and Aikin, K. C.: Single-particle measurements of midlatitude black carbon and light-scattering aerosols from the boundary layer to the lower stratosphere, *Journal of Geophysical Research-Atmospheres*, 111, Artn D16207 Doi 10.1029/2006jd007076, 2006.

Shen, Z., Liu, J., Horowitz, L. W., Henze, D. K., Fan, S., Levy, H., Mauzerall, D. L., Lin, J. T., and Tao, S.: Analysis of transpacific transport of black carbon during HIPPO-3: implications for black carbon aging, *Atmospheric Chemistry and Physics*, 14, 6315-6327, DOI 10.5194/acp-14-6315-2014, 2014.

Shindell, D. T., Chin, M., Dentener, F., Doherty, R. M., Faluvegi, G., Fiore, A. M., Hess, P., Koch, D. M., MacKenzie, I. A., Sanderson, M. G., Schultz, M. G., Schulz, M., Stevenson, D. S., Teich, H., Textor, C., Wild, O., Bergmann, D. J., Bey, I., Bian, H., Cuvelier, C., Duncan, B. N., Folberth, G., Horowitz, L. W., Jonson, J., Kaminski, J. W., Marmer, E., Park, R., Pringle, K. J., Schroeder, S., Szopa, S., Takemura, T., Zeng, G., Keating, T. J., and Zuber, A.: A multi-model assessment of pollution transport to the Arctic, *Atmospheric Chemistry and Physics*, 8, 5353-5372, 2008.

Textor, C., Schulz, M., Guibert, S., Kinne, S., Balkanski, Y., Bauer, S., Berntsen, T., Berglen, T., Boucher, O., Chin, M., Dentener, F., Diehl, T., Feichter, J., Fillmore, D., Ginoux, P., Gong, S., Grini, A., Hendricks, J., Horowitz, L., Huang, P., Isaksen, I. S. A., Iversen, T., Kloster, S., Koch, D., Kirkevåg, A., Kristjánsson, J. E., Krol, M., Lauer, A., Lamarque, J. F., Liu, X., Montanaro, V., Myhre, G., Penner, J. E., Pitari, G., Reddy, M. S., Seland, O., Stier, P., Takemura, T., and Tie, X.: The effect of harmonized emissions on aerosol properties in global models - an AeroCom experiment, *Atmospheric Chemistry and Physics*, 7, 4489-4501, 2007.

Tritscher, T., Juranyi, Z., Martin, M., Chirico, R., Gysel, M., Heringa, M. F., DeCarlo, P. F., Sierau, B., Prevot, A. S. H., Weingartner, E., and Baltensperger, U.: Changes of hygroscopicity and morphology during ageing of diesel soot, *Environ Res Lett*, 6, Artn 034026 Doi 10.1088/1748-9326/6/3/034026, 2011.

van der Werf, G. R., Randerson, J. T., Giglio, L., Collatz, G. J., Mu, M., Kasibhatla, P. S., Morton, D. C., DeFries, R. S., Jin, Y., and van Leeuwen, T. T.: Global fire emissions and the contribution of deforestation, savanna, forest, agricultural, and peat fires (1997-2009), *Atmospheric Chemistry and Physics*, 10, 11707-11735, DOI 10.5194/acp-10-11707-2010, 2010.

Vignati, E., Karl, M., Krol, M., Wilson, J., Stier, P., and Cavalli, F.: Sources of uncertainties in modelling black carbon at the global scale, *Atmospheric Chemistry and Physics*, 10, 2595-2611, 2010.

Wang, H. L., Rasch, P. J., Easter, R. C., Singh, B., Zhang, R. D., Ma, P. L., Qian, Y., Ghan, S. J., and Beagley, N.: Using an explicit emission tagging method in global modeling of source-receptor relationships for black carbon in the Arctic: Variations, sources, and transport pathways, *Journal of Geophysical Research-Atmospheres*, 119, 12888-12909, Doi 10.1002/2014jd022297, 2014.

Wang, Q., Jacob, D. J., Fisher, J. A., Mao, J., Leibensperger, E. M., Carouge, C. C., Le Sager, P., Kondo, Y., Jimenez, J. L., Cubison, M. J., and Doherty, S. J.: Sources of carbonaceous aerosols and deposited black carbon in the Arctic in winter-spring: implications for radiative forcing, *Atmospheric Chemistry and Physics*, 11, 12453-12473, 10.5194/acp-11-12453-2011, 2011.

Wofsy, S. C., Team, H. S., Team, C. M., and Team, S.: HIAPER Pole-to-Pole Observations (HIPPO): fine-grained, global-scale measurements of climatically important atmospheric gases and aerosols, *Philos T R Soc A*, 369, 2073-2086, DOI 10.1098/rsta.2010.0313, 2011.

Zarzycki, C. M., and Bond, T. C.: How much can the vertical distribution of black carbon affect its global direct radiative forcing?, *Geophysical Research Letters*, 37, Artn L20807 Doi 10.1029/2010gl044555, 2010.

Zhang, G. J., and Mcfarlane, N. A.: Sensitivity of Climate Simulations to the Parameterization of Cumulus Convection in the Canadian Climate Center General-Circulation Model, *Atmos Ocean*, 33, 407-446, 1995.

Zhang, R. Y., Khalizov, A. F., Pagels, J., Zhang, D., Xue, H. X., and McMurry, P. H.: Variability in morphology, hygroscopicity, and optical properties of soot aerosols during atmospheric processing, *P Natl Acad Sci USA*, 105, 10291-10296, DOI 10.1073/pnas.0804860105, 2008.

Table 1. Best-fit aging timescales for 13 regional BC tracers (units = hours), the ~~normalized~~-mean ~~normalized~~ absolute error (~~N~~MNAE) for the improved model (imp) and the original model (ori), and the ~~normalized~~-mean ~~normalized~~ bias (MNNMB) for the improved model compared to the vertical profiles measured by HIPPO.

		CA	SU	EU	MA	EA	ME	NA	SE	IN	AF	SA	AU	RR	<del>N</del> <u>M</u> <u>N</u> AE (imp)	<del>N</del> <u>M</u> <u>N</u> AE (ori)	* <u>M</u> <u>N</u> <u>N</u> MB (imp)
<b>HIPPO1</b>	Jan	200	90	120	120	4	12	160	4	4	4	4	4	90	3.8	26.2	0.04
<b>HIPPO2</b>	Nov	200	160	160	90	4	4	4	4	4	90	90	90	200	2.0	13.1	0.17
<b>HIPPO3</b>	Apr	200	200	200	200	38	200	4	38	27	24	24	24	200	1.5	6.1	-0.05
<b>HIPPO4</b>	Jun	60	4	160	12	4	160	4	4	4	4	4	4	200	1.1	10.6	0.11
<b>HIPPO5</b>	Aug	120	4	18	4	4	4	4	4	4	60	60	60	4	2.4	18.4	0.23

$$* \text{MNNB} = \frac{1}{N} \sum_{nlat} \sum_{nalt} \frac{BC_m(j,k) - BC_o(j,k)}{(BC_m(j,k) + BC_o(j,k))/2}$$

Table 2. Relative contribution (%) of emissions from thirteen source regions to BC burden in the troposphere (200-1000 hPa) over local and non-local receptors, and to over the central Pacific Ocean (PO, 160 °E-130 °W and 60 °S-58 °N). Relative contributions that are more than 10% are highlighted with gray shading.

		<u>Receptor</u>													
<u>—</u>	<u>—</u>	<u>CA</u>	<u>SU</u>	<u>EU</u>	<u>MA</u>	<u>EA</u>	<u>ME</u>	<u>NA</u>	<u>SE</u>	<u>IN</u>	<u>AF</u>	<u>SA</u>	<u>AU</u>	<u>RR</u>	<u>PO</u>
<u>Source</u>	<u>CA</u>	48.5	1.6	1.3	0.9	0.1	0.3	5.2	0.0	0.0	0.1	0.0	0.0	1.4	1.5
	<u>SU</u>	5.4	30.3	1.2	7.2	1.9	0.4	1.0	0.1	0.1	0.0	0.0	0.0	1.8	5.9
	<u>EU</u>	13.7	43.6	82.4	42.8	3.8	15.2	3.2	0.3	1.1	4.5	0.3	0.0	7.0	7.9
	<u>MA</u>	0.8	4.2	0.6	18.1	1.0	1.3	0.3	0.1	0.3	0.0	0.0	0.0	0.3	0.9
	<u>EA</u>	6.2	9.5	0.5	1.8	76.9	0.5	4.6	6.2	0.4	0.1	0.0	0.1	9.6	26.3
	<u>ME</u>	2.4	4.1	3.7	20.3	2.3	53.3	1.5	1.1	4.7	3.2	0.2	0.1	2.5	3.8
	<u>NA</u>	10.6	1.9	2.4	1.8	0.4	1.4	72.9	0.2	0.3	0.6	0.4	0.0	4.8	4.2
	<u>SE</u>	0.6	0.2	0.1	0.1	5.0	0.2	1.3	60.1	0.9	0.1	0.1	3.3	6.0	8.6
	<u>IN</u>	0.8	0.3	0.2	0.9	6.8	4.9	1.2	22.1	89.1	0.8	0.0	0.1	9.8	5.4
	<u>AF</u>	0.8	1.2	5.2	4.4	1.1	20.8	2.3	1.6	2.7	88.5	9.8	9.8	35.9	7.4
	<u>SA</u>	0.1	0.1	0.0	0.0	0.0	0.1	1.5	0.2	0.0	1.2	88.2	5.7	11.6	6.5
	<u>AU</u>	0.0	0.0	0.0	0.0	0.0	0.0	0.0	5.3	0.0	0.0	0.2	79.1	3.4	7.0
	<u>RR</u>	9.9	3.1	2.4	1.7	0.7	1.5	5.0	2.8	0.5	0.8	0.8	1.8	6.0	14.7

		<u>Receptor</u>													
<u>—</u>	<u>—</u>	<u>NA</u>	<u>CA</u>	<u>EA</u>	<u>SU</u>	<u>EU</u>	<u>AF</u>	<u>SA</u>	<u>IN</u>	<u>AU</u>	<u>MA</u>	<u>SE</u>	<u>ME</u>	<u>RR</u>	<u>PO</u>
<u>Source</u>	<u>NA</u>	72.9	10.6	0.4	1.9	2.4	0.6	0.4	0.3	0.0	1.8	0.2	1.4	4.8	4.2
	<u>CA</u>	5.2	48.5	0.1	1.6	1.3	0.1	0.0	0.0	0.0	0.9	0.0	0.3	1.4	1.5
	<u>EA</u>	4.6	6.2	76.9	9.5	0.5	0.1	0.0	0.4	0.1	1.8	6.2	0.5	9.6	26.3
	<u>SU</u>	1.0	5.4	1.9	30.3	1.2	0.0	0.0	0.1	0.0	7.2	0.1	0.4	1.8	5.9



<b>EU</b>	3.2	13.7	3.8	43.6	82.4	4.5	0.3	1.1	0.0	42.8	0.3	15.2	7.0	7.9
<b>AF</b>	2.3	0.8	1.1	1.2	5.2	88.5	9.8	2.7	9.8	4.4	1.6	20.8	35.9	7.4
<b>SA</b>	1.5	0.1	0.0	0.1	0.0	1.2	88.2	0.0	5.7	0.0	0.2	0.1	11.6	6.5
<b>IN</b>	1.2	0.8	6.8	0.3	0.2	0.8	0.0	89.1	0.1	0.9	22.1	4.9	9.8	5.4
<b>AU</b>	0.0	0.0	0.0	0.0	0.0	0.0	0.2	0.0	79.1	0.0	5.3	0.0	3.4	7.0
<b>MA</b>	0.3	0.8	1.0	4.2	0.6	0.0	0.0	0.3	0.0	18.1	0.1	1.3	0.3	0.9
<b>SE</b>	1.3	0.6	5.0	0.2	0.1	0.1	0.1	0.9	3.3	0.1	60.1	0.2	6.0	8.6
<b>ME</b>	1.5	2.4	2.3	4.1	3.7	3.2	0.2	4.7	0.1	20.3	1.1	53.3	2.5	3.8
<b>RR</b>	5.0	9.9	0.7	3.1	2.4	0.8	0.8	0.5	1.8	1.7	2.8	1.5	6.0	14.7

Table 3. Global budget for BC emitted from thirteen source regions (2009-2011 average) using the optimized aging timescale for each region.

	CA	SU	EU	MA	EA	ME	NA	SE	IN	AF	SA	AU	RR	All
<b>Emission (Tg/yr)</b>	0.07	0.14	0.46	0.03	1.93	0.17	0.35	0.55	0.75	1.62	0.64	0.15	0.12	6.98
<b>Dry Dep (Tg/yr)</b>	0.01	0.02	0.11	0.01	0.23	0.03	0.05	0.04	0.14	0.24	0.09	0.02	0.02	1.00
<b>Wet Dep (Tg/yr)</b>	0.06	0.12	0.35	0.02	1.70	0.14	0.30	0.51	0.61	1.38	0.55	0.13	0.10	5.98
<b>Burden (Gg)</b>	1.2	1.7	9.0	0.6	11.4	4.3	3.6	4.7	10.7	31.6	9.1	2.2	2.8	92.8
<b>Lifetime (d)</b>	6.3	4.4	7.1	7.1	2.2	9.3	3.7	3.1	5.2	7.1	5.2	5.3	8.4	4.9

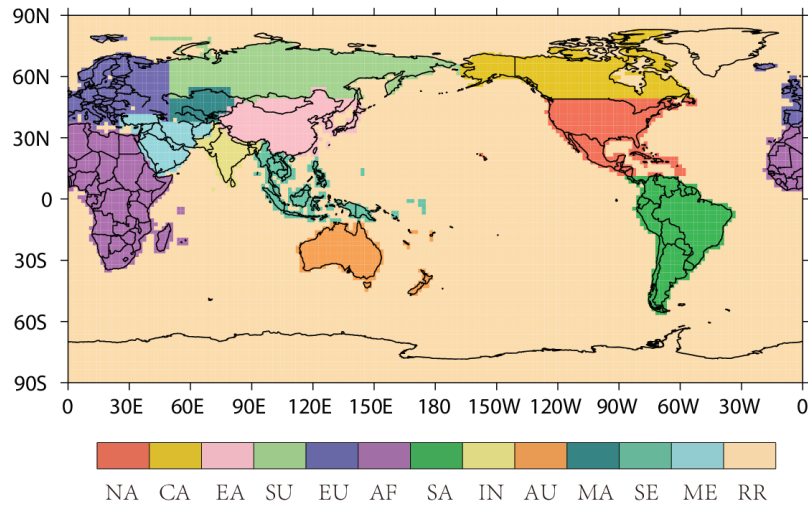


Figure 1. The thirteen defined source regions: Canada (CA), North America except Canada (NA), East Asia (EA), the former Soviet Union (SU), Europe (EU), Africa (AF), South America (SA), India (IN), Australia (AU), Middle Asia (MA), Southeast Asia (SE), the Middle East (ME), and the rest regions (RR).

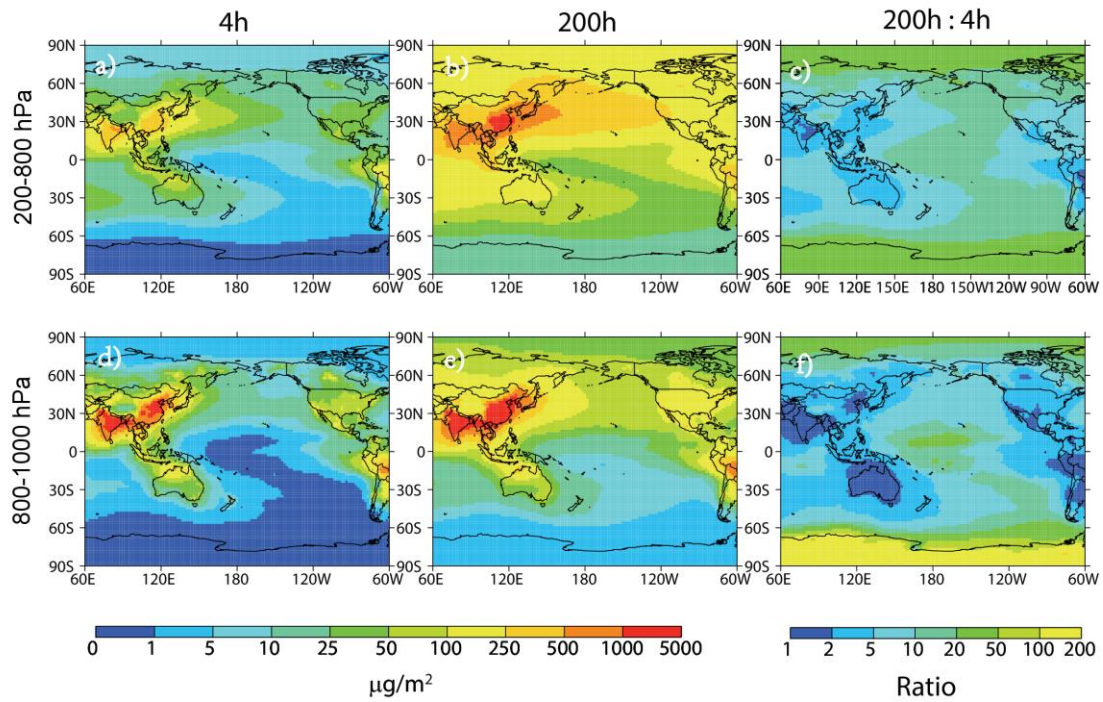


Figure 2. The annual averaged (2009-2011) column burden of BC at 200-800 hPa (a, b) and 800-1000 hPa (d, e) when aging timescale is 4 h (a, d) and 200 h (b, e). The ratio of BC burden for simulations with aging timescale of 200 h and 4 h is in (c) and (f).

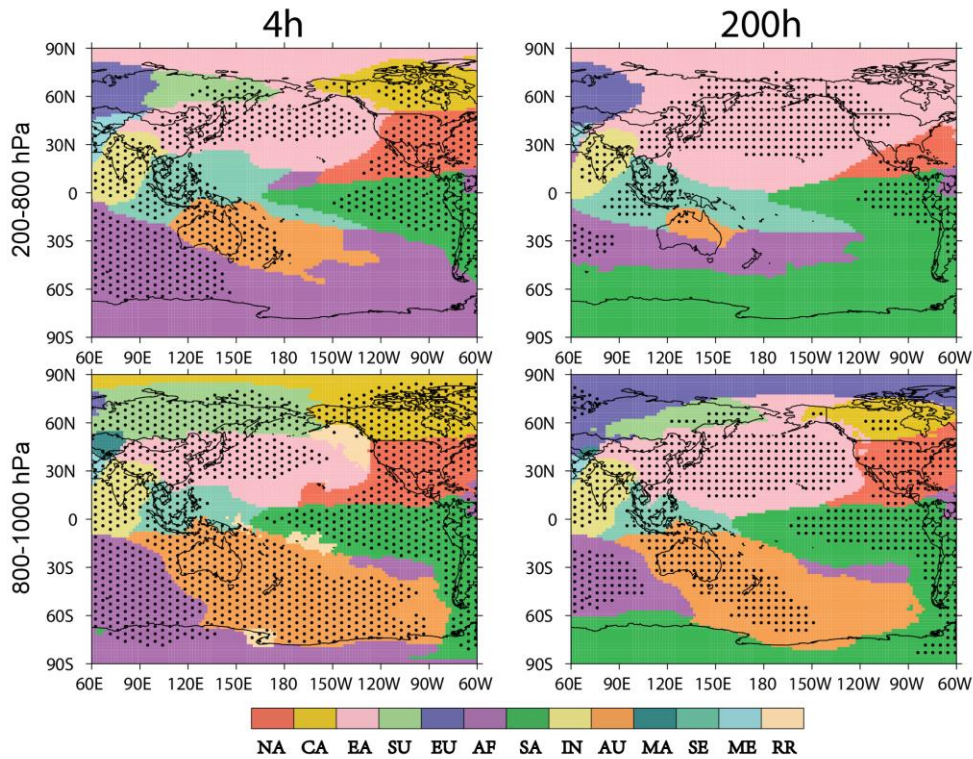
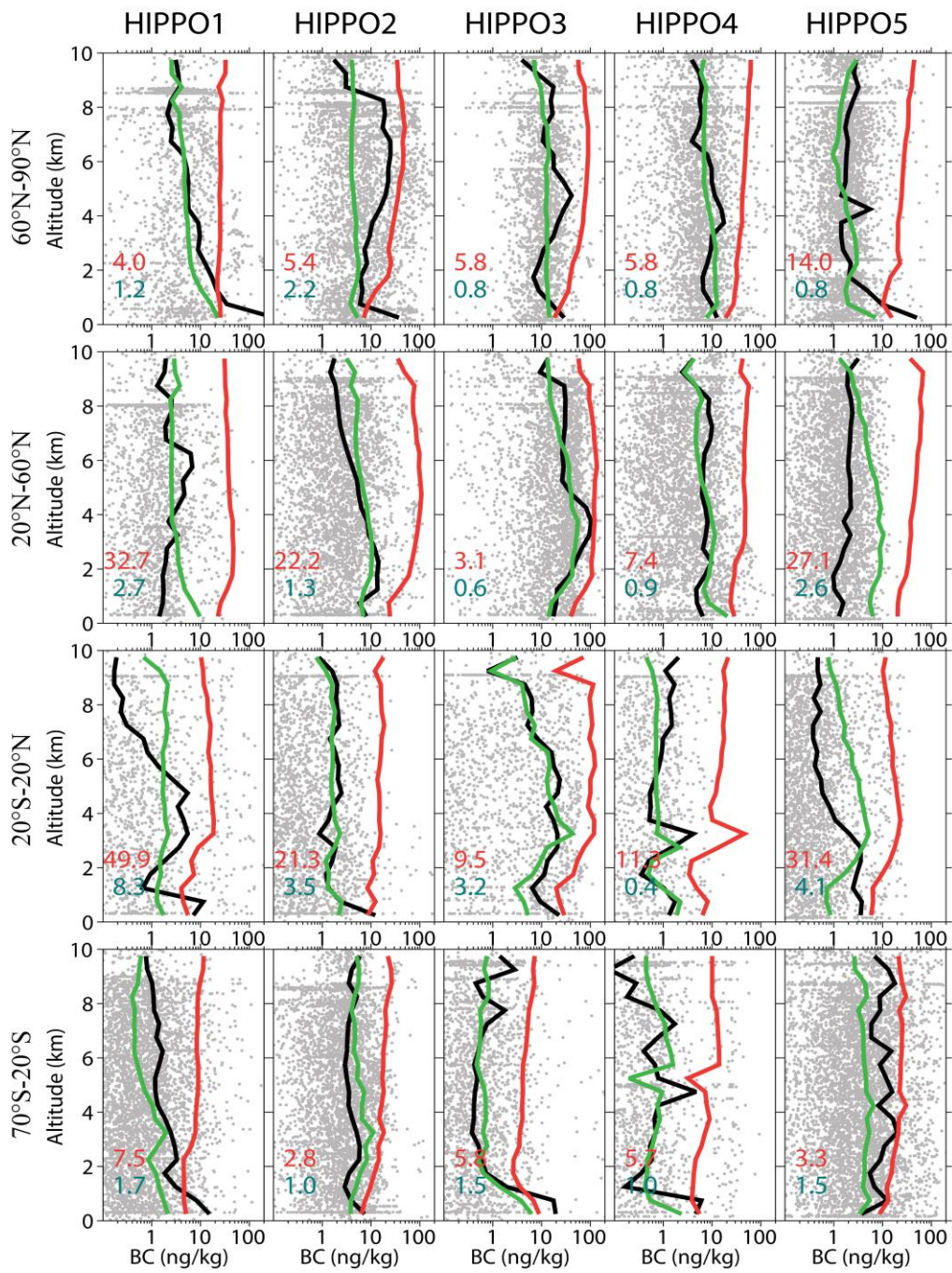


Figure 3. The dominant regional contributors to the annual averaged (2009-2011) column burden of BC at 200-800 hPa (top) and 800-1000 hPa (bottom) when aging timescale is 4 h (left) and 200 h (right). Dotted areas are where the dominant contributors account for more than 50% of the total BC burden.





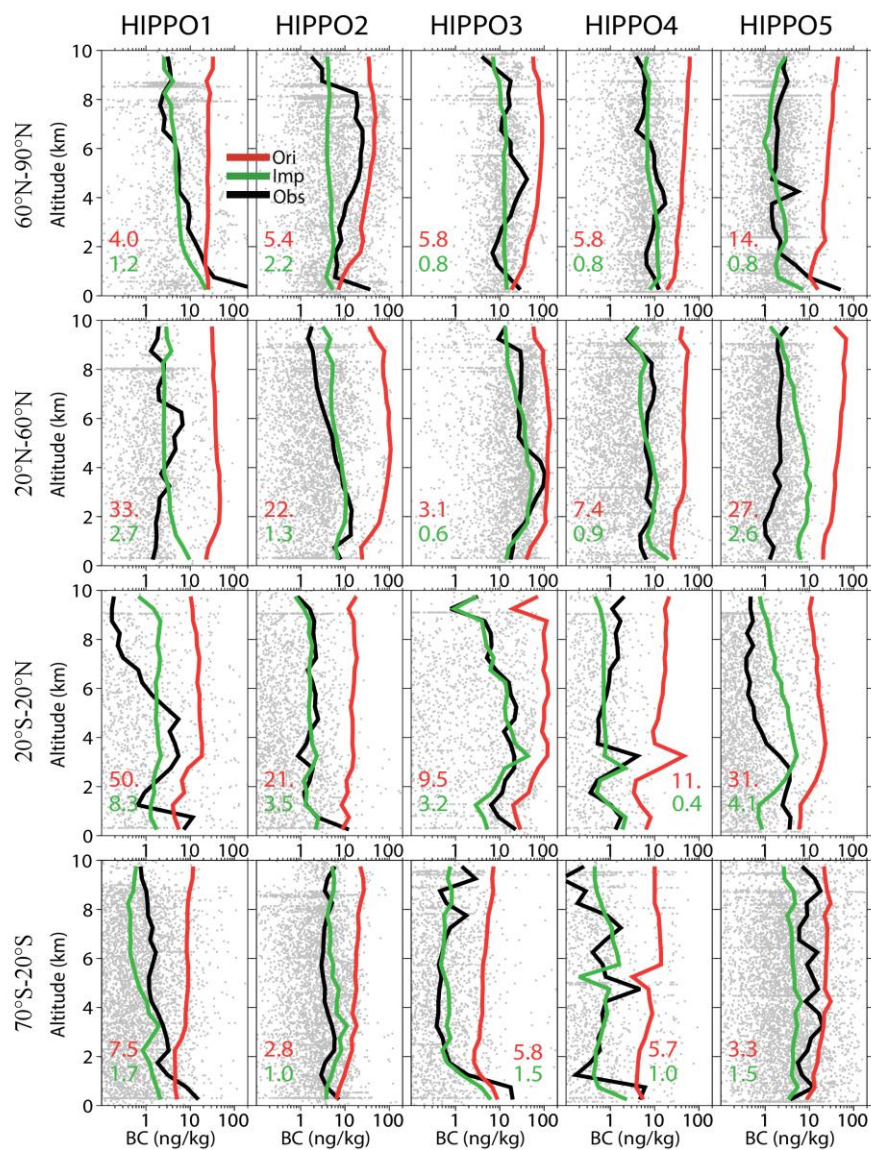


Figure 4. Vertical profiles of simulated and observed BC mass mixing ratios over 0.5 km altitude bins along the flight tracks of HIPPO 1-5 over the central Pacific Ocean (130 W-160 E). Data are shown separately as averaged over 70 S-20 S, 20 S-20 N, 20 N-60 N, and 60 N-90 N. The black, red, and green lines are mean values of BC mixing ratios from observations, default, and improved models, respectively. The gray dots represent measured BC concentrations. The green (red) number indicates the averaged  $\overline{NMNAE}$  for the improved (original) model (see Equation 3).

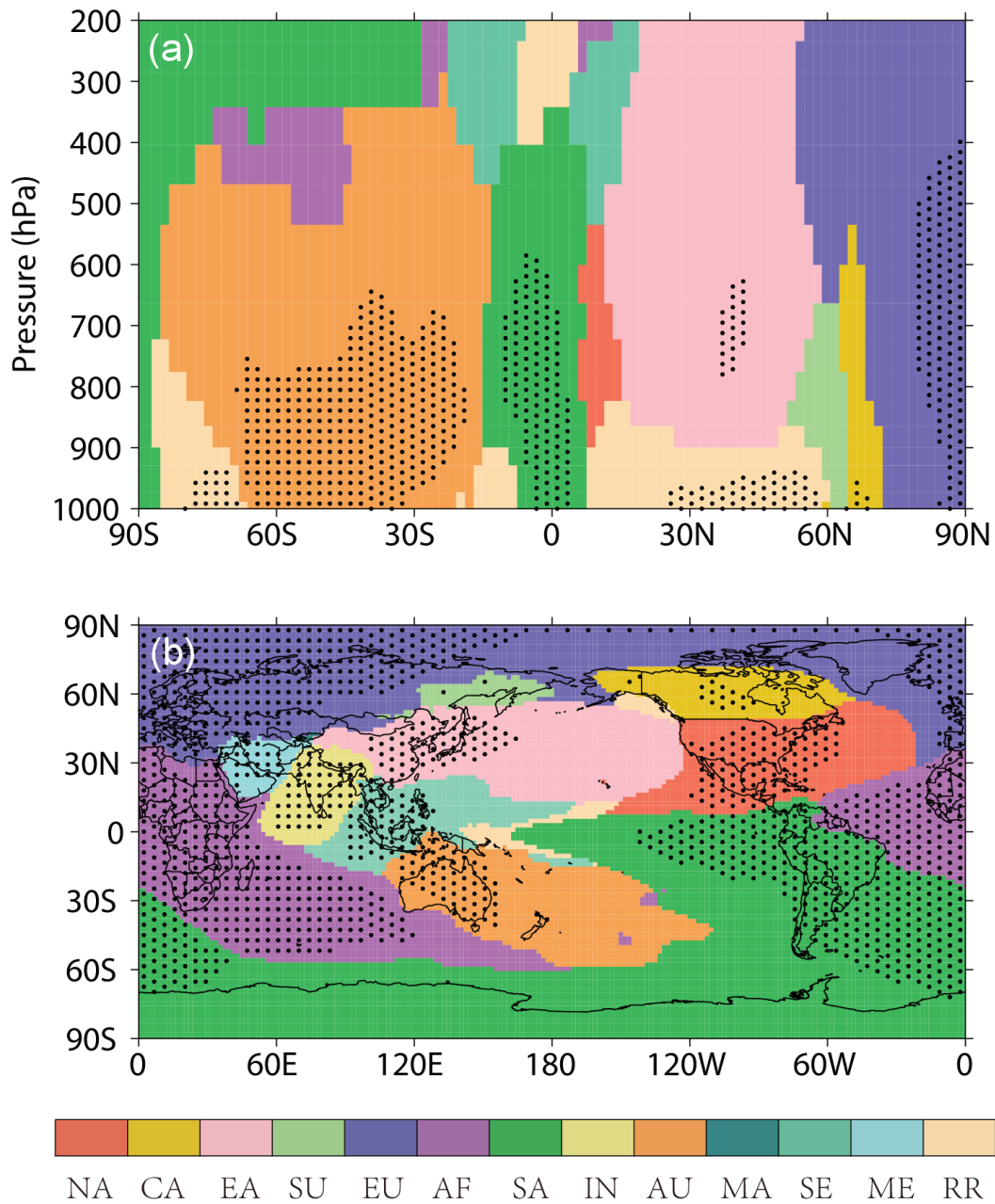


Figure 5. The most significant regional contributors to (a) zonal mean BC concentration over the Pacific (130°W-160°E), and (b) the column burden of BC in the troposphere (200-1000 hPa, 2009-2011 average). Dotted area represents where the most significant contributor accounts for more than 50% of the total BC.



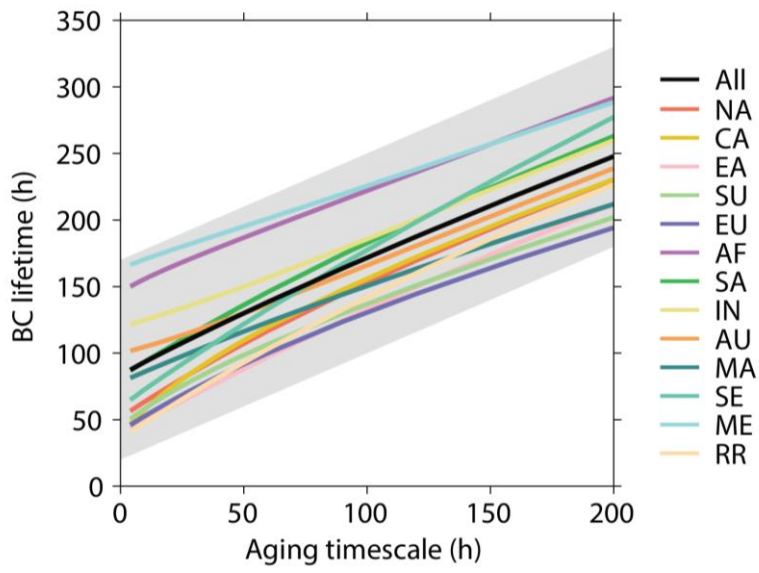


Figure 6. The lifetime of global BC (black) and tagged BC emitted from 13 source regions (colors) as a function of aging timescale. The top and bottom edges of the grey shading indicate a slope of 0.8.